Electronic Supplementary Material (ESI) for ChemComm.

Electronic Supporting Information

Exploring Mitochondrial Targeting: Innovative Fluorescent Probe Reveals Nernstian Potential and Partitioning Combination

Javier Ordóñez-Hernández,[a] Daniela Ceballos-Ávila,[a] Fernando H. Real,[b] Luis B. Tovar-Y-Romo,[b] and Arturo Jiménez-Sánchez [a,*]

[a] Instituto de Química, Universidad Nacional Autónoma de México, Circuito Exterior S.N., Ciudad Universitaria, Coyoacán, México, D.F. 04510, México.

[b] Instituto de Fisiología Celular, Universidad Nacional Autónoma de México, Circuito Exterior S.N., Ciudad Universitaria, Coyoacán, México, D.F. 04510, México.

To whom correspondence should be addressed. Email: arturo.jimenez@iquimica.unam.mx

Table of contents

1. Experimental section…… S1

1.1 Materials and reagents…… S1

1.2 Cell culture and confocal imaging…… S1

1.3 Partition coefficient (P) determination…… S2

1.4 Self-association partition formalism…… S2

1.5 Synthesis…… …… S3

2. Nuclear magnetic resonance spectra…… S6

3. High-resolution mass spectra…… S14

4. Absorption and emission fluorescence spectra…… S16

5. Confocal microscopy…… S23

6. Acknowledgements…… S26

1. Experimental section

1.1 Materials and reagents

All starting materials were purchased from Aldrich and used without further purification. Solvents were dried by standard methods or distilled prior to use. Reactions were monitored by TLC on precoated silica gel plates (ALUGRAM SIL G/UV254) and revealed by exposure to a UV254 lamp. Infrared spectra were obtained using a Perkin-Elmer Spectrum 400 FT-IR/FT-FIR spectrophotometer, wavenumber is reported in cm^{-1}. ^{1}H and ^{13}C NMR spectra were recorded on a Jeol Eclipse-300 MHz, and Bruker Avance III 400 MHz model spectrometers using $CDCl_3$ and CD_3SOCD_3 as solvents. Data for ^{1}H NMR is reported as follows: Chemical shift as parts per million downfield (δ) from solvent reference (CDCl3 δ 7.26 for 1H, δ 77.1 for 13C), integration, multiplicity (s=singlet, d = doublet, t = triplet, q = quartet, m = multiplet, br = broad). High-resolution DART+ mass spectra were obtained on a Jeol JMS-T100LC spectrometer and values of the signals are expressed in mass/charge units (m/z), followed by the relative intensity with reference to a 100% base peak. Fluorescence experiments were measured on a FS5 spectrofluorometer from Edinburgh Instruments, UV-Vis absorption spectra were taken on a Thermo Scientific Evolution diode array UV-Vis spectrophotometer.

1.2 Cell Culture and Confocal Imaging

HeLa cells as well as live human pulmonary adenocarcinoma epithelial cells (SK-Lu-1) were cultured in RPMI-1640 medium (RPMI Medium 1640 (1x), Gibco, Gaithersburg MD) supplemented with 10% fetal bovine serum (FBS, Invitrogen, Carlsbad CA), L- glutamine (2 µM), penicillin G (100 u/mL), streptomycin sulfate (100 µg/ mL) at 37°C with 5% v/v CO_2. Live SK-LU-1 cells were seeded on 8 Petri dishes of 5 cm diameter with glass bottom for 36 hours before experiments using RPMI-1640 medium supplemented. Then, specific concentrations of **AztecM** and **AztecM-LD** 1 to 8 µM were used. Commercial specific organelle localizers were added on each Petri dish 45 minutes before imaging experiments. All dishes were washed two times with RPMI. During confocal imaging, microscope parameters were maintained constant and excitation light was fully-shielded to prevent laser artefacts.

For confocal imaging, live cells were seeded in 8 well µ–slides (iBidi, Germany) at a density of 20000 cells per well one day prior to experiments in MEM alpha with 10% FBS. On treatment day, cells were washed once in MEM alpha with no FBS and incubated with 1 to 8 µM **AztecM** and **AztecM-LD** probes for 30 minutes. For experiments with MitoLiteBlue®, 50 nM were added 10 minutes before **AztecM** and **AztecM-LD**. Cells were then washed twice in MEM alpha with no FBS and imaged maintaining 5% CO_2 and 37°C during the experiments using an inverted Zeiss LSM 880 microscope upgraded with an incubator or a Nikon A1R upgraded with a spectral detector unit. Additionally, high-resoltiuon confocal imaging using Airyscan technique available on the Carl Zeiss LSM 880 microscope was used to image mitochondrial network [Figs. 3 and 4, main text]. To avoid cell autofluorescence signal contamination, laser powers were maintained at 0.05 mW (0.2% from a 25 mW laser) and untreated cells were first recorded in order to subtract any native emission signal. On treatment day for fluorescence time course experiments, cells were incubated with 1 µM of the probes for 30 minutes in MEM alpha with 5% FBS for the indicated time at 37°C with 5% CO_2, then imaged at the same conditions using 100nM nigericin, 150 nM CCCP (after 5 min) and 5 mg/mL oligomycin A at 20 min.

1.3 Partition coefficient (P) determination.

Partition coefficient (*P*) were measured through octanol partitioning using a modified shake-flask method. Initially, 100 mL aliquots of the probe solution at 300 mM concentration in Tris buffer (10 mM, pH 7.4) and 1-octanol (Aldrich) were added to a 0.5 mL microtube. Tris buffer was utilized to maintain physiological pH during the measurement of *P* values for the probes. The tubes were then vortexed for 1 minute and centrifuged. Subsequently, 25 mL of each layer was extracted and diluted in 3 : 1 methanol : Tris or methanol : octanol solution to achieve a final composition of 3:1:1 methanol : octanol : Tris. An additional 4-fold dilution was performed for the aqueous layer. Three dilutions were prepared for each layer, and 100 mL of each dilution was pipetted into a 96-well plate. Absorbance readings were taken at 488 nm and 625 nm wavelengths. The mean absorbance at 500 nm (A_{500}) was calculated for each layer. The ratio of A_{500} of the organic layer to A_{500} of the aqueous layer provided the partition coefficient (*P*). All absorbance measurements were conducted within the linear range of the instrument.

1.4 Self-Association partition formalism

To demonstrate the self-association partition, we used the K. A. Connors formalism.[K. A. Connors, *Binding Constants. The Measurement of Molecular Complex Stability*, John Wiley & Sons, 1987, p. 411.] Let suppose that a substrate S associates to form aggregates S_m in phase 1 (aqueous phase). Phase 2 is the *probe or lipid phase* where only monomer species partitions into it, with partition coefficient $P_0 = [S]_2 / [S]_1$, for the general equilibria:

$$S_1 + S_1 + \ldots = S_m \tag{1}$$

With:

$$\beta_m = \frac{[S_m]_1}{[S_m]_1^m} \tag{2}$$

where S_1, S_2, …, S_m refer to the monomeric, dimeric and *m*-meric aggregated species in the aqueous phase, and β_1, β_2 and β_m refer to the respective association constants. Then, K. A. Connors proposed the following general scheme for relating the observed partition coefficient for a substrate S between and organic phase where only the monomer is present, and the aqueous phase in which association occurs:

$$\frac{P_0}{P} = 1 + \frac{2\beta_2[S]_2}{P_0} + \frac{3\beta_3[S]_2^2}{P_0^2} + \cdots + \frac{m\beta_m[S]_2^{m-1}}{P_0^{m-1}} \tag{3}$$

where *P* and P_0 are the observed and intrinsic partition coefficients [*P* = (org. conc) / (aq. conc)], respectively. The simplest form of self-association is the dimer formation in the aqueous phase, *m* = 2, then eq (3) yields:

$$\frac{P_0}{P} = 1 + \frac{2\beta_2[S]_2}{P_0} \tag{4}$$

where β_2 is the partition dimerization constant.

1.5 Synthesis

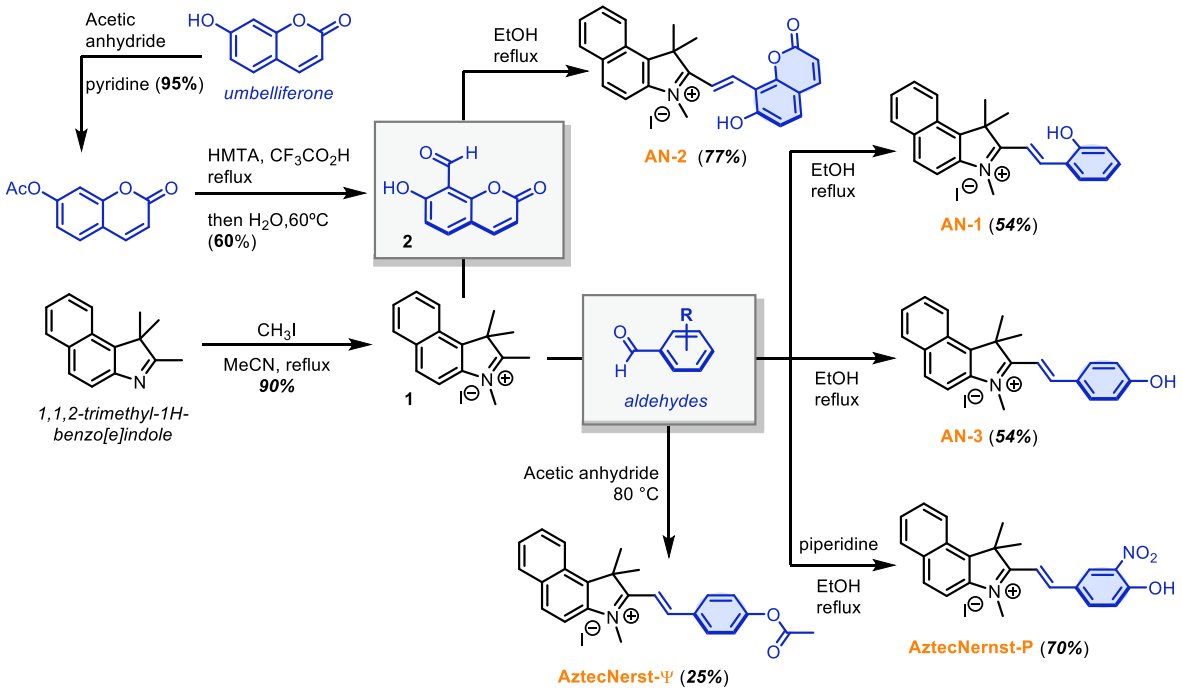

Scheme S1. Synthesis of **AztecNernst** probes.

Synthesis of 1,1,2,3-tetramethyl-1H-benzo[e]indol-3-ium iodide (**1**)

To a solution of 1,1,2-trimethylbenz[e]indole (1 g, 4.78 mmol) in acetonitrile (30 mL) was added methyl iodide (1.02g, 7.17 mmol) and the reaction mixture was refluxed for 12 h. The resulting white solid was filtered under vacuum, washed with Et_2O, and dried to yield 1.51 g (90%) of indolium salt(**1**). ^{1}H NMR (300 MHz, CD_3SOCD_3, δ, ppm): 8.37 (d, J=8.4 Hz, 1H), 8.29 (d, J=8.9, 1H), 8.21 (d, J=7.8 Hz, 1H), 8.12 (d, J=8.9 Hz, 1H), 7.81-7.69 (m, 2H), 4.11 (s, 3H), 2.90 (s, 3H), 1.80 (s, 6H). ^{13}C NMR (75 MHz, CD_3SOCD_3, δ, ppm): 196.5, 140.1, 137.1, 133.6, 131.1, 130.3, 129.0, 127.7, 124.0, 113.8, 55.8, 35.9, 21.9, 14.9.

Synthesis of 2-oxo-2*H*-chromen-7-yl acetate (**2**)

To a solution of 7-hydroxicoumarin (0.5 g, 3.08 mmol) in dichloromethane (10 mL) were added acetic anhydride (1 mL, 15 mmol) and pyridine (0.1 mL, 1.24 mmol). The reaction mixture was stirred under an argon atmosphere at room temperature for over 16 hours. Then, the volatiles were removed under reduced pressure and the residue was poured into water (10 mL) and extracted with ethyl acetate (15 mL) twice. The organic phase was dried over anhydrous sodium sulfate and evaporated in vacuo to obtain 2-oxo-2*H*-chromen-7-yl acetate as a white solid (0.6 g, 95%). ^{1}H NMR (300 MHz, $CDCl_3$, δ, ppm): 7.70 (d, *J*=9.6 Hz, 1H), 7.48 (d, *J*=8.4 Hz, 1H), 7.11 (d, J=2.2 Hz, 1H), 7.04

(dd, J_1=8.4 Hz, J_2=2.2 Hz, 1H), 6.39 (d, J=9.6 Hz, 1H), 2.30 (s, 3H). ^{13}C NMR (75 MHz, $CDCl_3$, δ, ppm): 168.7, 160.3, 154.7, 153.1, 128.6, 118.4, 116.7, 116.1, 110.4, 21.1.

Synthesis of 7-hydroxy-2-oxo-2H-chromene-8-carbaldehyde (**3**).

To an ice-cold solution of compound **2** (0.5 g, 2.44 mmol) in TFA (10 mL) was added hexamethylenetetramine (0.68 g, 4.88 mmol). The reaction mixture was refluxed for 16 hours and then was cooled down to room temperature, the volatiles were removed under reduced pressure, and water (10 mL) was added to the residue which was heated at 60 °C for 30 minutes. The suspension was then cooled to room temperature and the solid was filtered and washed with water which gave pure compound **4** as a beige solid (0.27 g, 60%). ^{1}H NMR (300 MHz, $CDCl_3$, δ, ppm): 12.21 (s, 1H), 10.59 (s, 1H), 7.65 (d, *J*=9.6 Hz, 1H), 7.59 (d, *J*=8.9 Hz, 1H), 6.88 (d, *J*=8.9 Hz, 1H), 6.32 (d, *J*=9.6 Hz, 1H). ^{13}C NMR (75 MHz, $CDCl_3$, δ, ppm): 192.9, 165.5, 159.1, 156.7, 143.4, 136.0, 114.7, 113.4, 110.8, 106.6

Synthesis of **AN-2**

A solution of compound **4** (0.05 g, 0.263 mmol), and compound **1** (0.092 g, 0.263 mmol) in absolute ethanol (7 mL) was heated to reflux for 16 h. The reaction was then cooled down to room temperature, the resulting orange solid was filtered, washed with ethanol, and dried to give 106 mg (77%) of **AN-2**. IR (ATR, cm^{-1}): 3447, 1727, 1661, 1520, 1472, 1404, 1349, 1260, 1020. ^{1}H NMR (300 MHz, CD_3SOCD_3, δ, ppm): 8.60 (d, J=16.7 Hz, 1H), 8.50 (d, J=8.6 Hz, 1H), 8.31 (d, J=9.0 Hz, 1H), 8.22 (d, J=7.8 Hz, 1H), 8.16 (d, J=1.6 Hz, 1H), 8.12 (d, J=9.5 Hz, 1H), 8.08 (d, J=9.5 Hz), 7.81-7.70 (m, 3H), 7.07 (d, J=8.6 Hz, 1H), 6.42 (d, J=9.5 Hz, 1H), 4.18 (s, 3H), 2.02 (s, 6H). ^{13}C NMR (75 MHz, $CDCl_3$, δ, ppm):182.9, 162.0, 159.3, 154.6, 144.9, 140.5, 139.5, 138.0, 134.0, 133.2, 130.9, 130.0, 128.4, 127.2, 126.7, 123.3, 115.5, 113.3, 113.2, 112.1, 111.7, 109.0, 53.5, 34.8, 25.6. HRMS (ESI-TOF): calcd. for $C_{26}H_{22}NO_3$: 396.15997, found: 396.15930 (1.68 ppm).

Synthesis of **AN-1**

This compound was obtained as described for **AN-2**, using *o*-hydroxybenzaldehyde (0.05 g, 0.409 mmol), and compound **1** (0.144 g, 0.409 mmol) in absolute ethanol (7 mL). The product was obtained as an orange solid (0.1 g, 54%). IR (ATR, cm^{-1}): 3300, 3123, 1592, 1251.^{1}H NMR (300 MHz, $CDCl_3$, δ, ppm): 11.05 (s, 1H), 8.59 (d, J=16.6 Hz, 1H), 8.45 (d, J=8.4 Hz, 1H), 8.30 (d, J=9.0 Hz, 1H), 8.22 (d, J=8.2 Hz, 1H), 8.17 (d, J=8.2 Hz, 1H), 8.11 (d, J=9.0 Hz, 1H), 7.83-7.69 (m, 3H), 7.48 (t, J=8.4 Hz, 1H), 7.06 (d, J=8.2 Hz, 1H), 7.01 (d, J=7.5 Hz, 1H), 4.22 (s, 3H), 1.99 (s, 6H). ^{13}C NMR (75 MHz, CD_3SOCD_3, δ, ppm): 183.1, 159.4, 147.6, 140.1, 138.4, 135.8, 133.7, 131.5, 130.6, 130.3, 129.0, 127.7, 127.2, 123.7, 121.9, 120.6, 117.3, 113.9, 112.2, 54.1, 35.5, 26.3. HRMS (DART+): calcd. for $C_{23}H_{22}NO^+$: 328.17014, found: 328.16944 (2.13 ppm).

Synthesis of **AN-3**

This compound was obtained as described for **AN-2**, Using *p*-hydroxybenzaldehyde (0.05 g, 0.409 mmol), and compound **1** (0.144 g, 0.409 mmol) in absolute ethanol (7 mL). The product was obtained as an orange solid (0.11 g, 54%). IR (ATR, cm^{-1}): 3300, 3195, 1573, 1531, 1268, 1167. ^{1}H NMR (300 MHz, CD_3SOCD_3, δ, ppm): 8.44 (d, J=16.3 Hz, 1H), 8.40 (d, J=8.4 Hz, 1H), 8.27 (d, J=9.0 Hz, 1H), 8.20 (d, J=8.4 Hz, 1H), 8.14 (d, J=8.7 Hz, 2H), 8.07 (d, J=9 Hz, 1H), 7.79 (t, J=8.2 Hz, 1H), 7.70 (t, J=8.2 Hz, 1H), 7.50 (d, J=16.3 Hz, 1H), 6.98 (d, J=8.7 Hz, 1H), 4.21 (s, 3H), 2.00 (s, 6H). ^{13}C NMR (75 MHz, CD_3SOCD_3, δ, ppm):182.9, 163.4, 153.2, 140.1, 138.0, 134.0, 133.6, 131.3, 130.6, 128.9, 127.5, 127.3, 126.7, 123.6, 116.9, 113.7, 109.5, 54.0, 26.9. HRMS (DART+)): calcd. for $C_{26}H_{22}NO_3^+$: 328.17014, found: 328.16972 (1.27 ppm).

Synthesis of **AztecNerst-P**

This compound was obtained as described for **AN-2**, using 4-hydroxy-3-nitrobenzaldehyde (0.05 g, 0.299 mmol), compound **1** (0.105 g, 0.299 mmol) and piperidine (30 µL, 0.299 mmol) in absolute ethanol (7 mL). The product was obtained as a violette solid (0.1 g, 70%). IR (ATR, cm^{-1}): 3054, 2977, 1621, 1588, 1557, 1261.^{1}H NMR (300 MHz, $CDCl_3$, δ, ppm): 8.59 (s, 1H), 8.38 (d, J=15.4 Hz, 1H), 8.30 (d, J=8.3 Hz, 1H), 8.15 (d, J=8.9 Hz, 1H), 8.11 (d, J=8.3 Hz, 1H), 8.00 (bs, 1H), 7.86 (d, J=8.9 Hz, 1H), 7.74-7.68 (m, 1H), 7.57-7.55 (m, 1H), 6.95 (d, J=15.4 Hz, 1H), 6.46 (d, J=9.3 Hz, 1H), 3.95 (s, 3H), 1.96 (s, 6H). ^{13}C NMR (75 MHz, CD_3SOCD_3, δ, ppm): 179.5, 172.2, 153.2, 140.5, 135.4, 132.6, 130.9, 130.5, 128.5, 127.7, 126.1, 123.1, 116.7, 112.8, 102.1, 52.3, 33.2, 26.8. HRMS (DART+): calcd. for $C_{23}H_{21}N_2O_3^+$: 373.15522, found: 373.15467 (1.46 ppm).

Synthesis of **AztecNernst-Ψ**

This compound was obtained as described for AN-2, using 4-hydroxy-3-benzaldehyde (0.05 g, 0.409 mmol), and compound **1** (0.144 g, 0.409 mmol) in acetic anhydride (7 mL). The product was obtained as an orange solid (0.05 g, 25%). IR (ATR, cm^{-1}): 3150, 1762, 1614, 1595, 1577, 1540, 1198.^{1}H NMR (300 MHz, $CDCl_3$, δ, ppm): 8.50 (d, J=16.5 Hz, 1H), 8.43 (d, J=8.5 Hz, 1H), 8.30 (d, J=8.5 Hz, 2H), 8.29 (s, 1H), 8.22 (d, J=7.9 Hz, 1H), 8.12 (d, J=8.9 Hz, 1H), 7.82 (t, J=7.1 Hz, 1H), 7.73 (t, J=7.1 Hz, 1H), 7.72 (d, J=16.5 Hz, 1H), 7.38 (d, J=8.5 Hz, 2H), 4.29 (s, 3H), 2.32 (s, 3H), 2.01 (s, 6H).^{13}C NMR (75 MHz, CD_3SOCD_3, δ, ppm): 183.1, 169.7, 154.5, 151.3, 140.0, 138.8, 133.8, 132.8, 132.3, 131.5, 130.6, 129.1, 127.9, 127.2, 123.8, 123.4, 114.0, 113.4, 54.5, 35.8, 25.5, 21.5. HRMS (DART+): calcd. for $C_{25}H_{24}NO_2^+$: 373.18070, found: 370.18064 (0.16 ppm).

2. Nuclear Magnetic Resonance Spectra

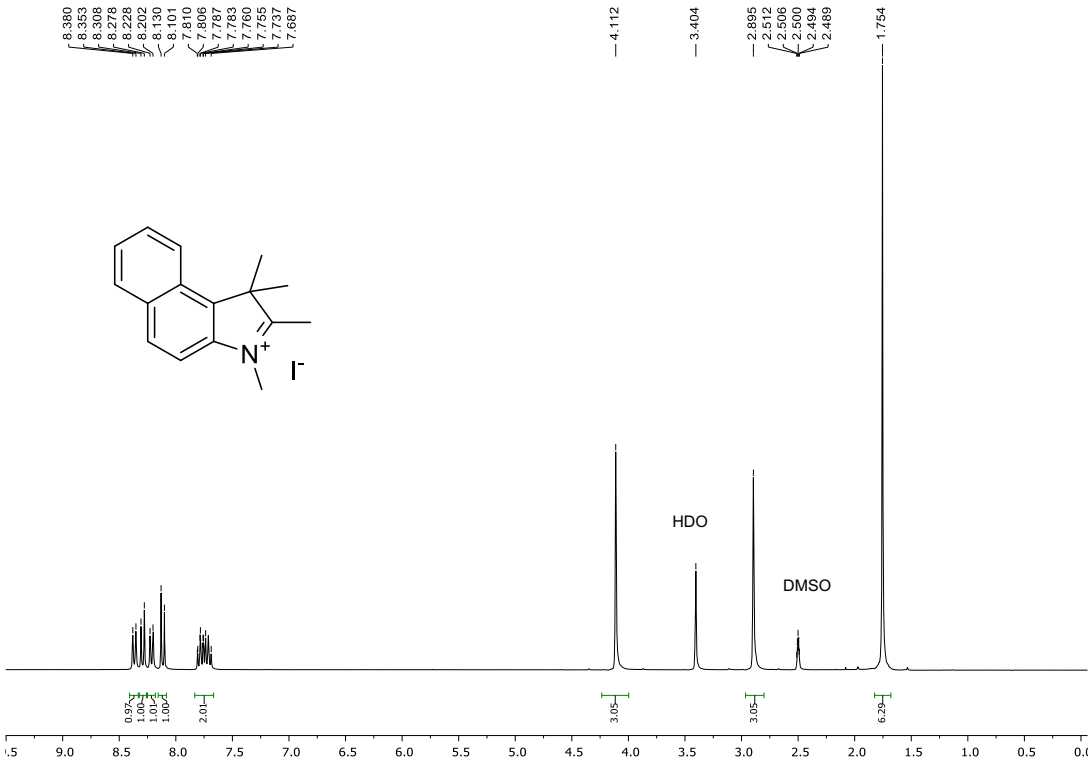

Figure S1. ^{1}H NMR spectrum of compound **1** at 300 MHz in CD_3SOCD_3

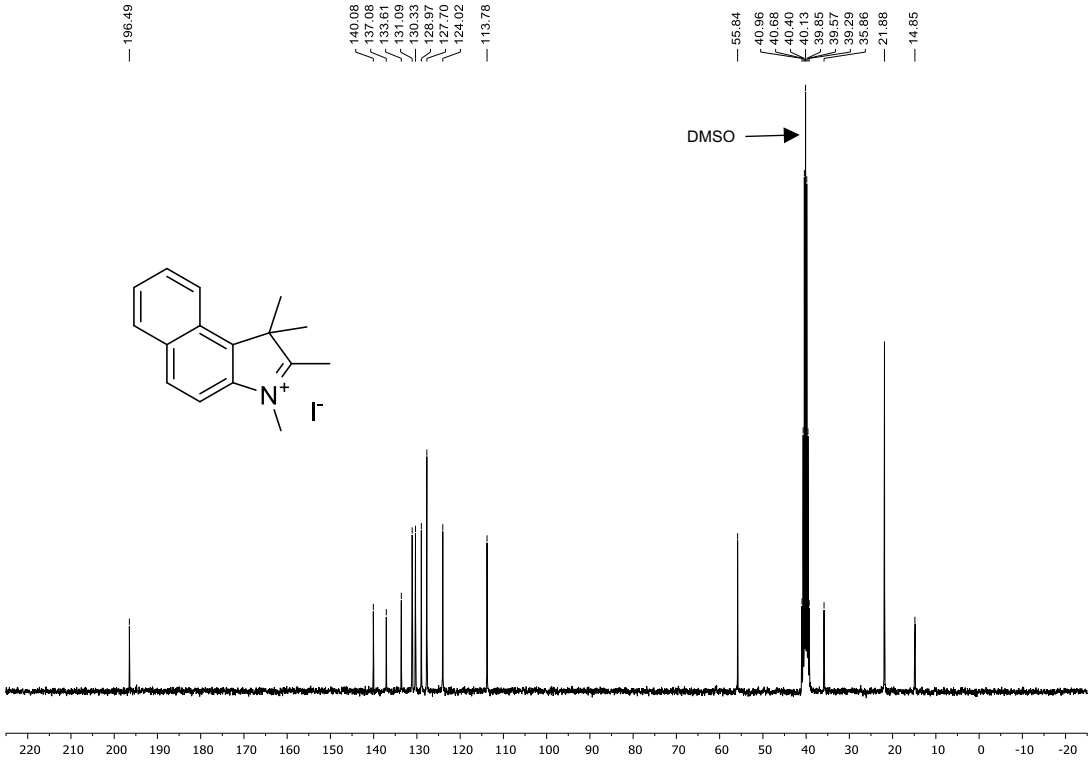

Figure S2. ^{13}C NMR spectrum of compound **1** at 75 MHz in CD_3SOCD_3

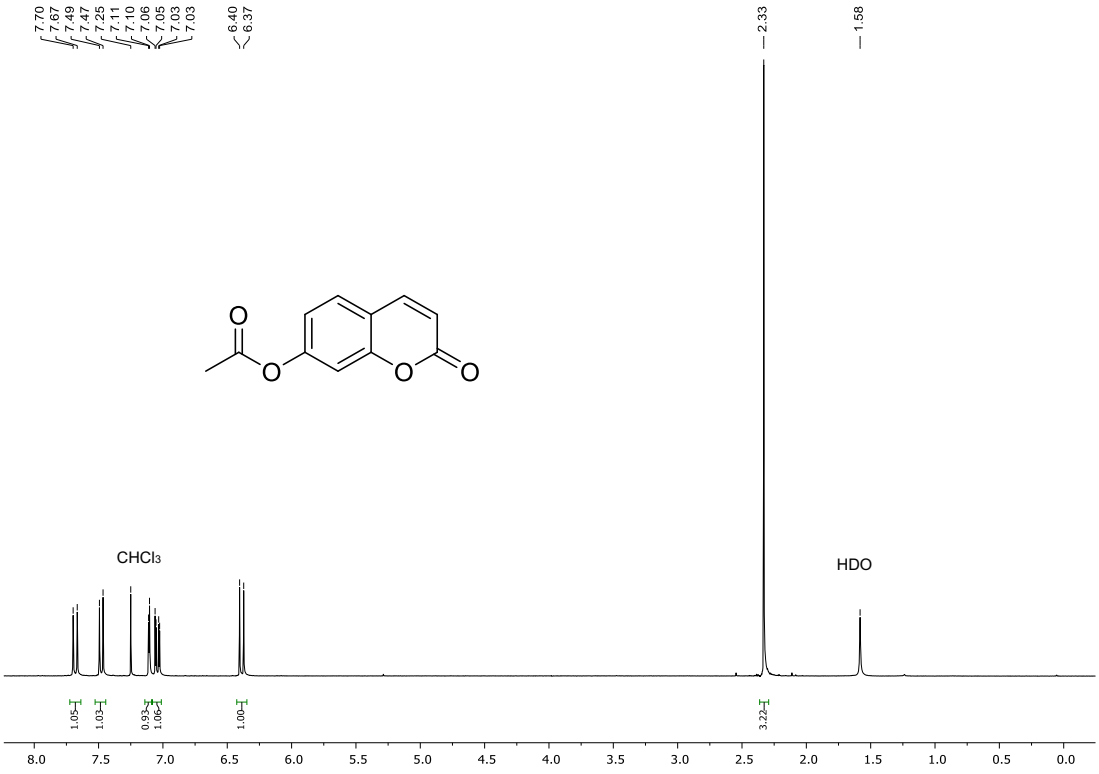

Figure S3. ^{1}H NMR spectrum of compound **2** at 300 MHz in $CDCl_3$

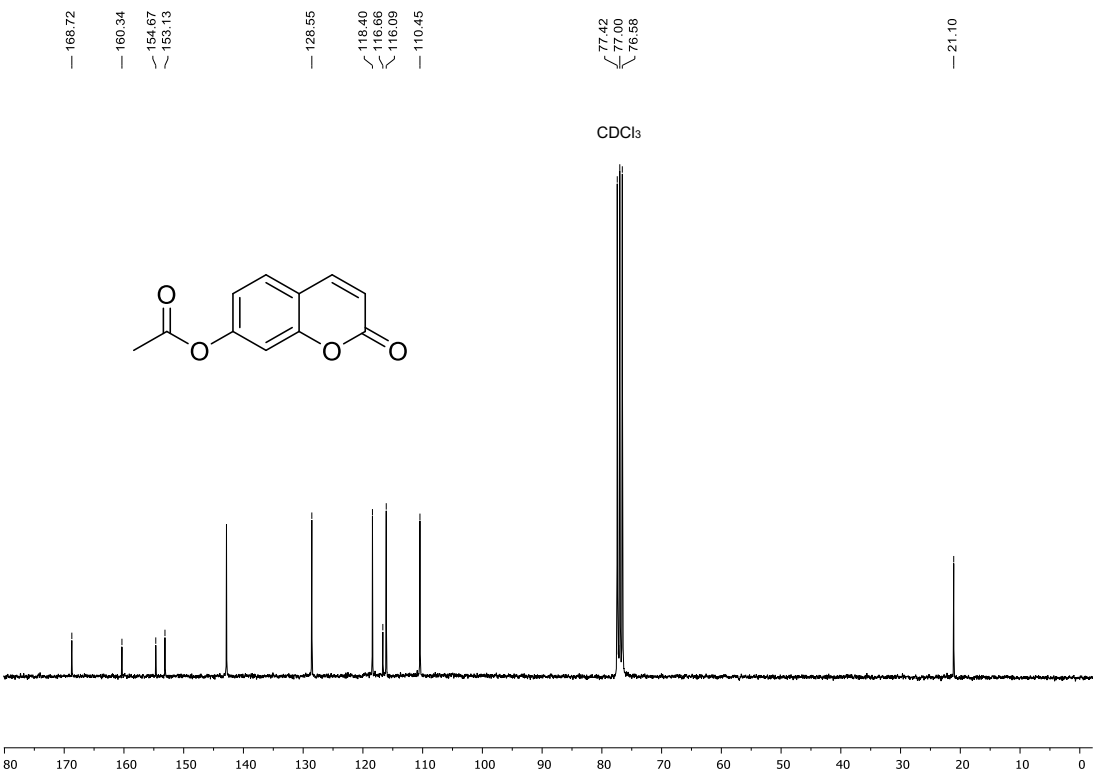

Figure S4. ^{13}C NMR spectrum of compound **2** at 75 MHz in $CDCl_3$

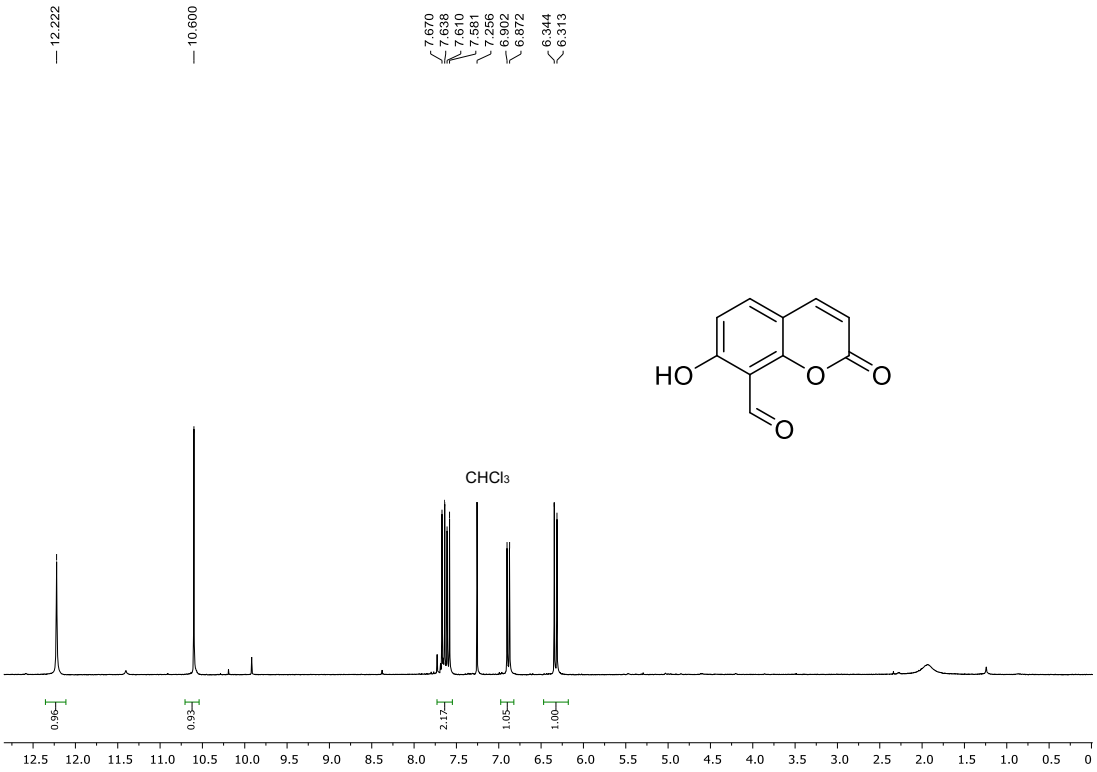

Figure S5. ^{1}H NMR spectrum of compound **3** at 300 MHz in $CDCl_3$

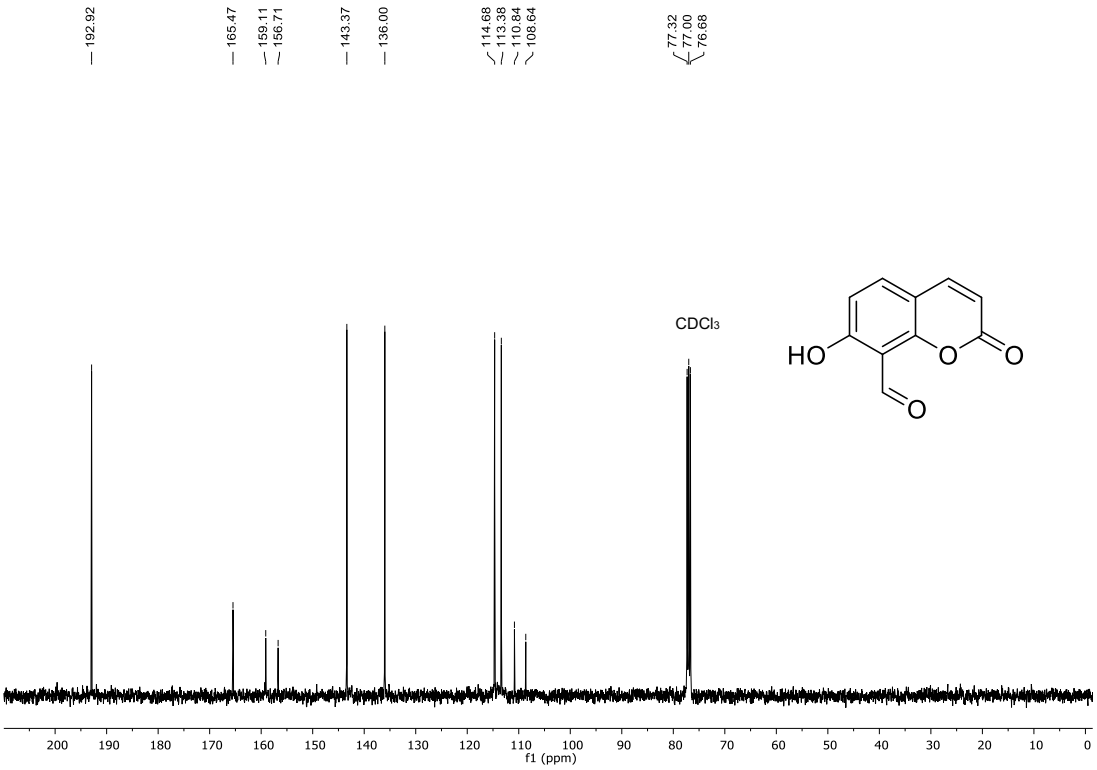

Figure S6. ^{13}C NMR spectrum of compound **3** at 75 MHz in $CDCl_3$

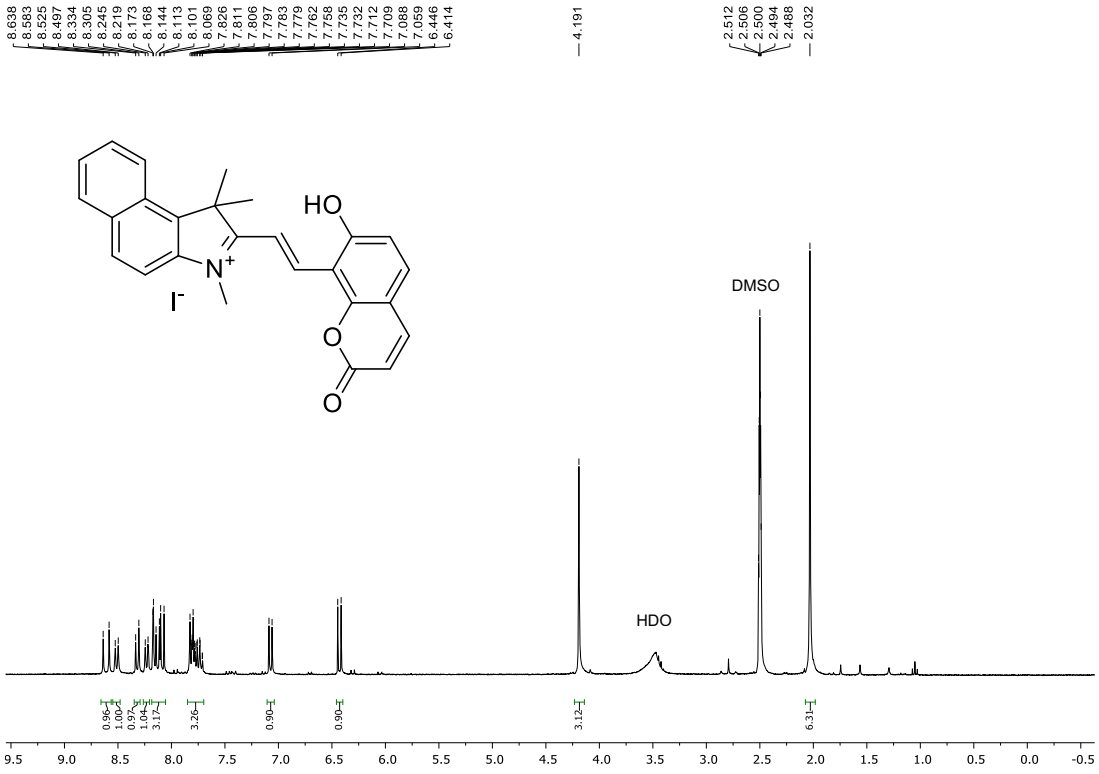

Figure S7. ^{1}H NMR spectrum of **AN-2** at 300 MHz in CD_3SOCD_3

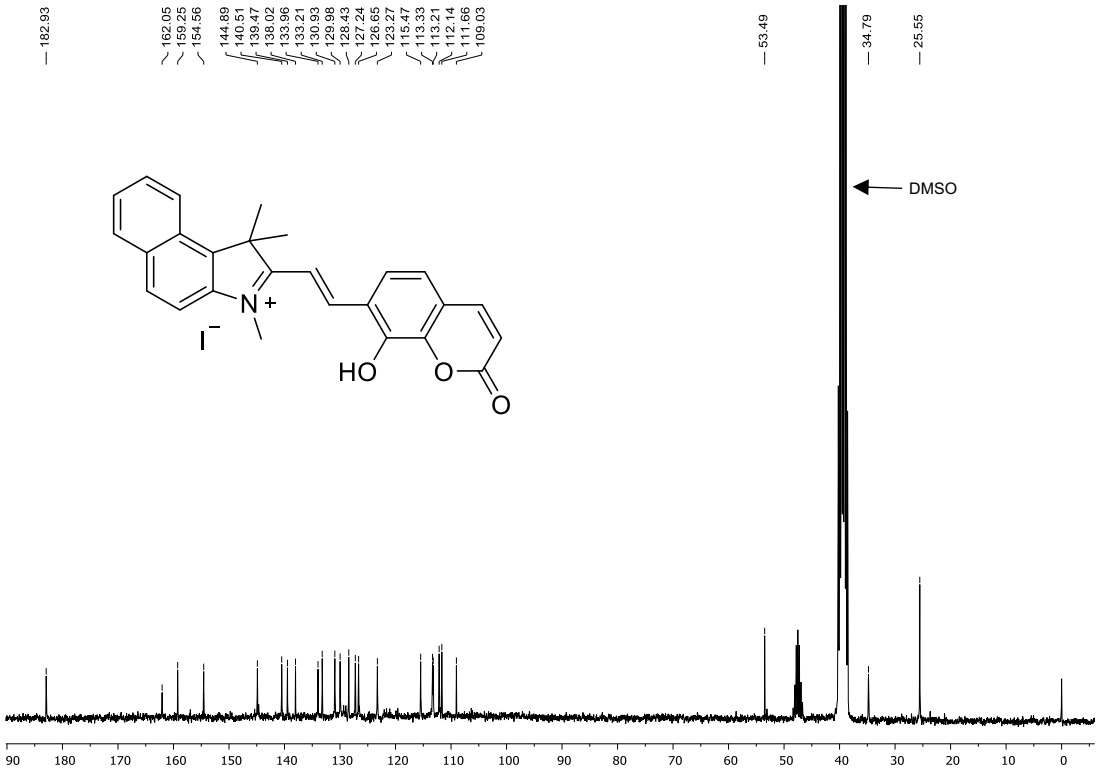

Figure S8. ^{13}C NMR spectrum of **AN-2** at 75 MHz in CD_3SOCD_3

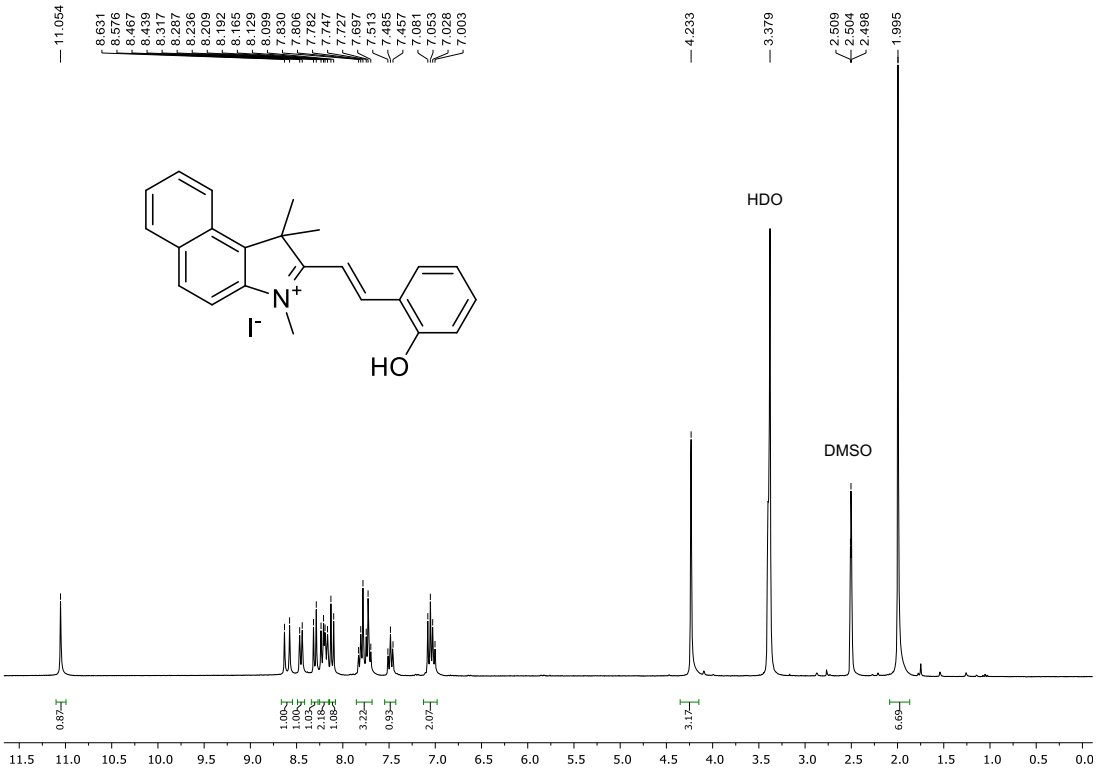

Figure S9. ^{1}H NMR spectrum of **AN-1** at 300 MHz in CD_3SOCD_3

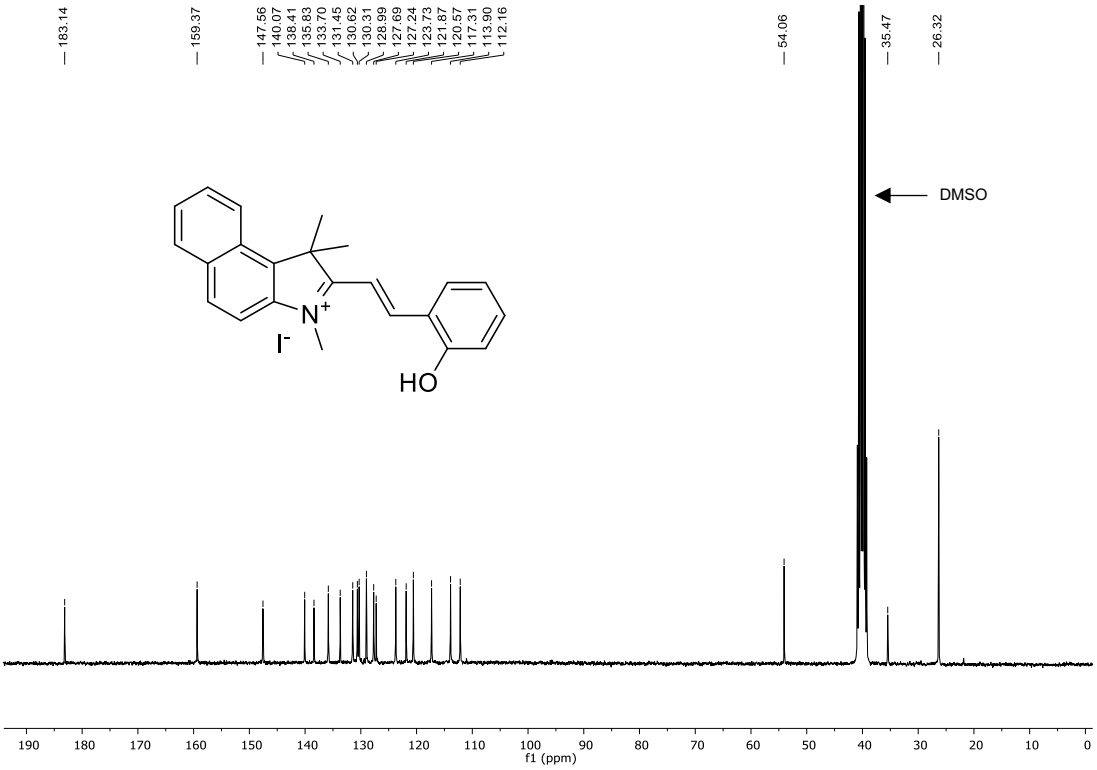

Figure S10. ^{13}C NMR spectrum of **AN-1** at 75 MHz in CD_3SOCD_3

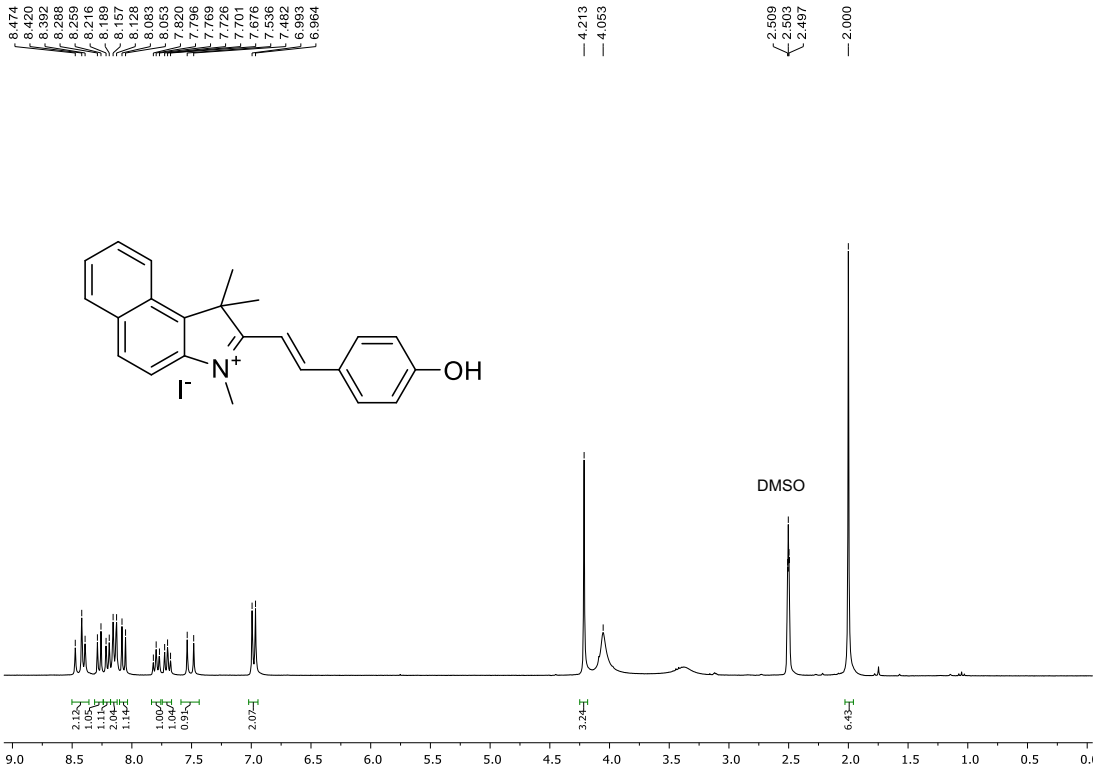

Figure S11. ^{1}H NMR spectrum of **AN-3** at 300 MHz in CD_3SOCD_3

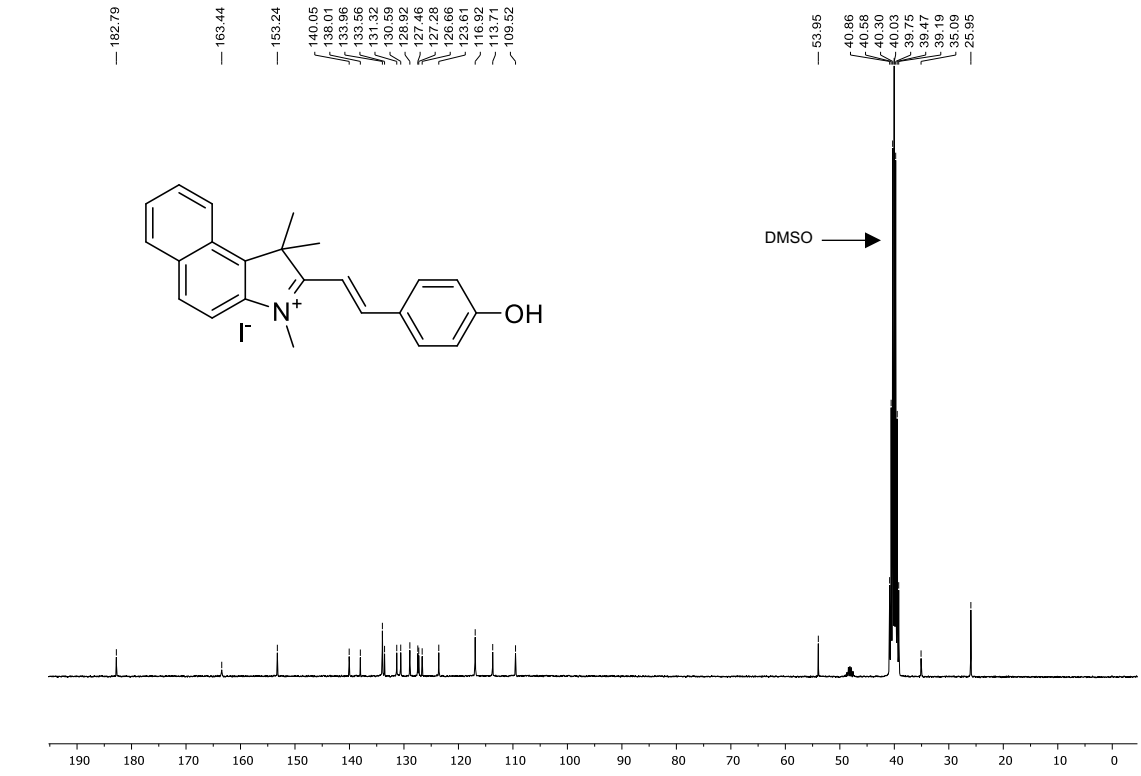

Figure S12. ^{13}C NMR spectrum of **AN-3** at 75 MHz in CD_3SOCD_3

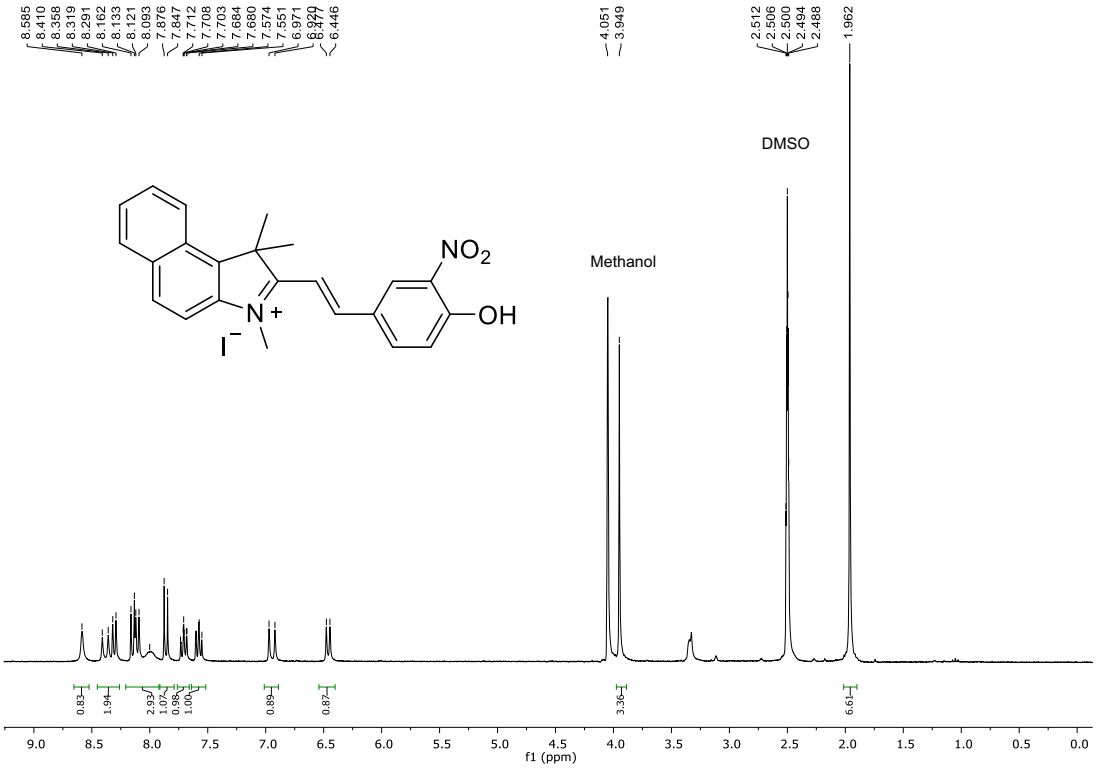

Figure S13. ^{1}H NMR spectrum of **AztecNernst-P** at 300 MHz in CD_3SOCD_3.

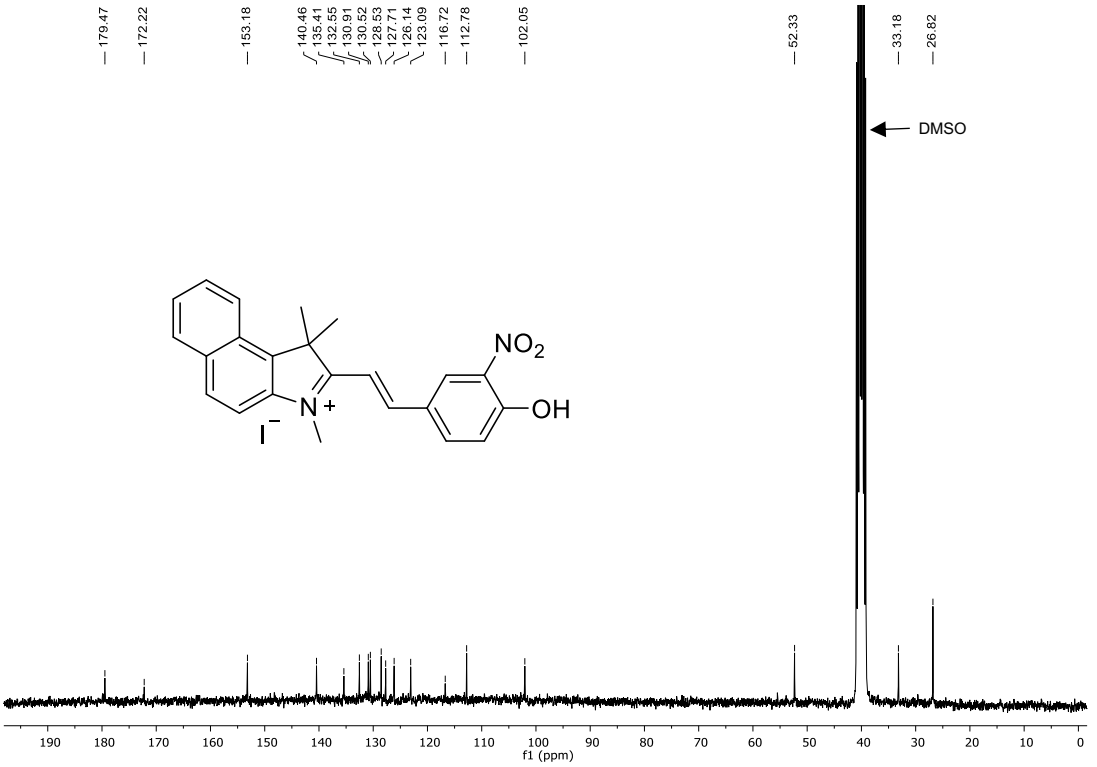

Figure S14. ^{13}C NMR spectrum of **AztecNernst-P** at 75 MHz in CD_3SOCD_3.

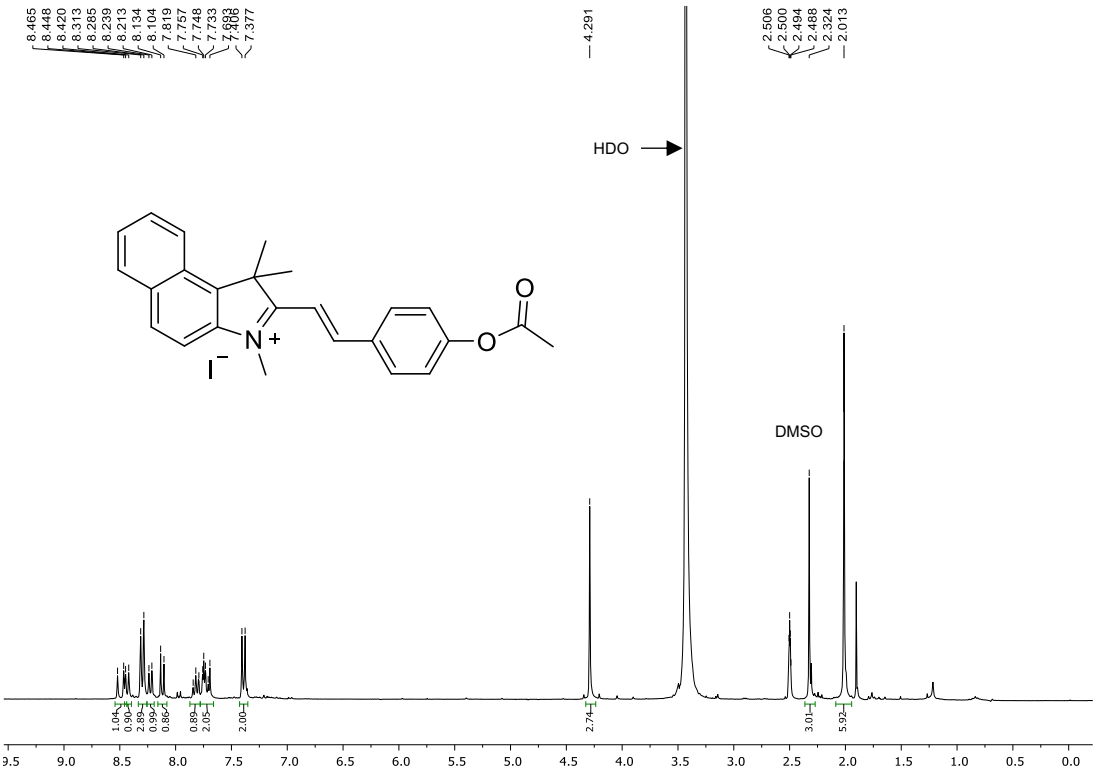

Figure S15. ^{1}H NMR spectrum of **Aztec Nernst-Ψ** at 300 MHz in CD_3SOCD_3.

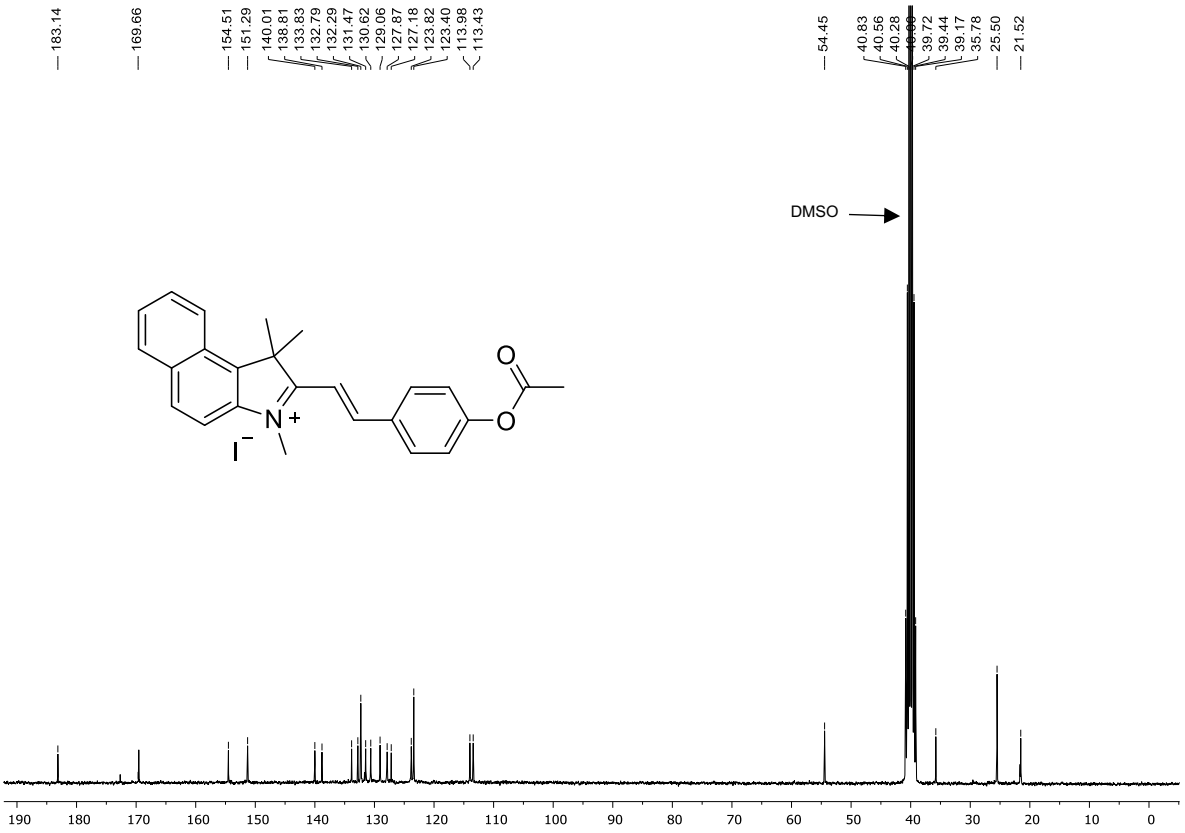

Figure S16. ^{13}C NMR spectrum of **AztecNernst-Ψ** at 75 MHz in CD_3SOCD_3

3. High-resolution mass spectra

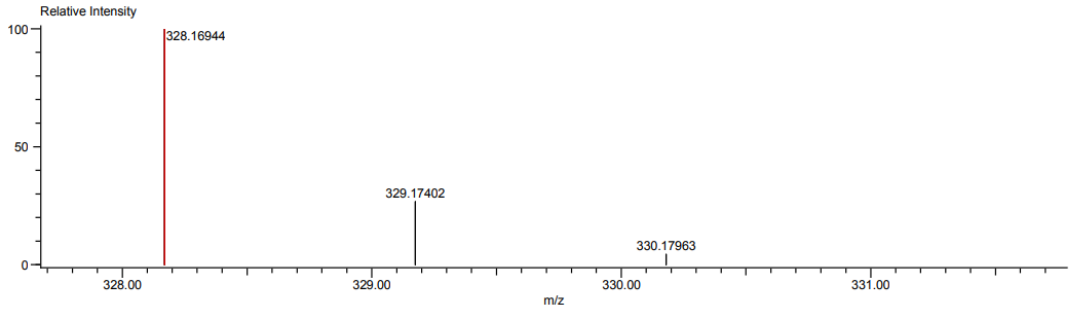

Mass	Intensity	Calc. Mass	Mass Difference (mmu)	Mass Difference (ppm)	Possible Formula	Unsaturation Number
328.16944	89812.19	328.17014	-0.70	-2.13	$^{12}C_{23}{}^{1}H_{22}{}^{14}N_{1}{}^{16}O_{1}$	13.5

Figure S17. High-resolution mass spectrum (DART+) of **AN-1**

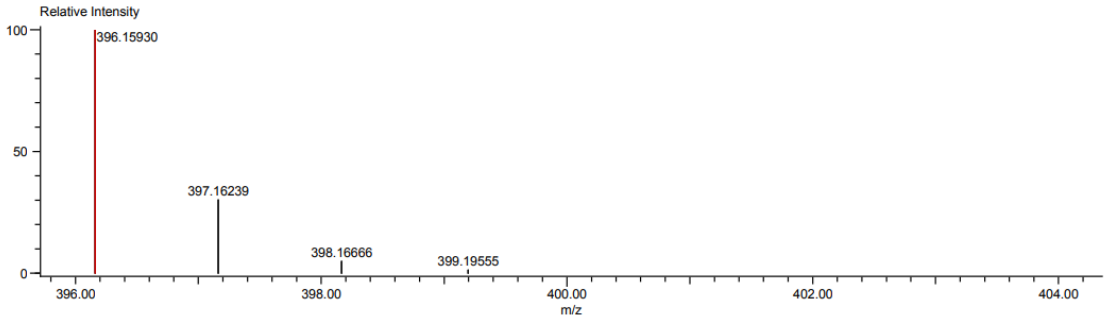

Mass	Intensity	Calc. Mass	Mass Difference (mmu)	Mass Difference (ppm)	Possible Formula	Unsaturation Number
396.15930	238765.63	396.15997	-0.66	-1.68	$^{12}C_{26}{}^{1}H_{22}{}^{14}N_{1}{}^{16}O_{3}$	16.5

Figure S18. High-resolution mass spectrum (DART+) of **AN-2**

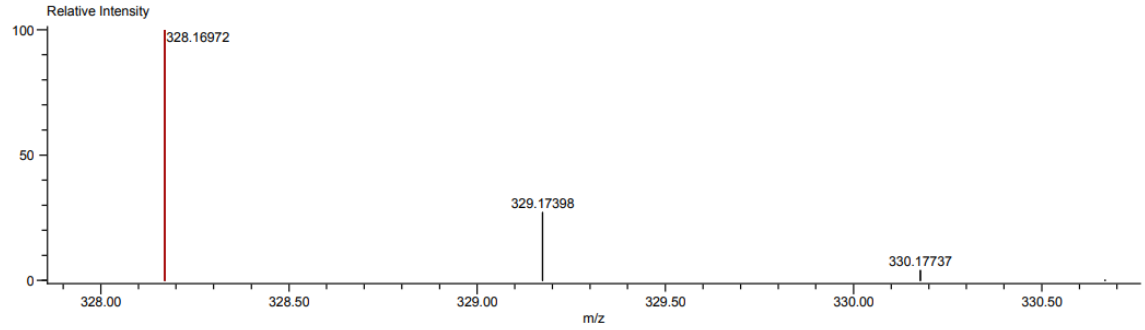

Mass	Intensity	Calc. Mass	Mass Difference (mmu)	Mass Difference (ppm)	Possible Formula	Unsaturation Number
328.16972	25395.13	328.17014	-0.42	-1.27	$^{12}C_{23}{}^{1}H_{22}{}^{14}N_{1}{}^{16}O_{1}$	13.5

Figure S19. High-resolution mass spectrum (DART+) of **AN-3**

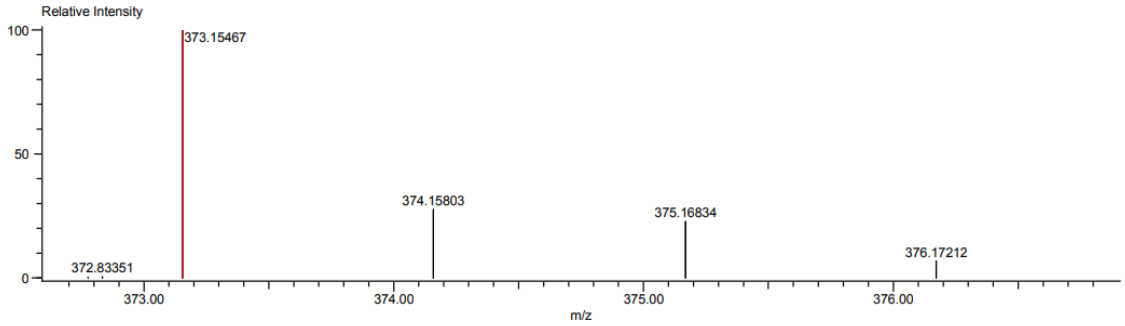

Mass	Intensity	Calc. Mass	Mass Difference (mmu)	Mass Difference (ppm)	Possible Formula	Unsaturation Number
373.15467	27962.33	373.15522	-0.54	-1.46	$^{12}C_{23}{}^{1}H_{21}{}^{14}N_{2}{}^{16}O_{3}$	14.5

Figure S20. High-resolution mass spectrum (DART+) of **AztecNernst-P**

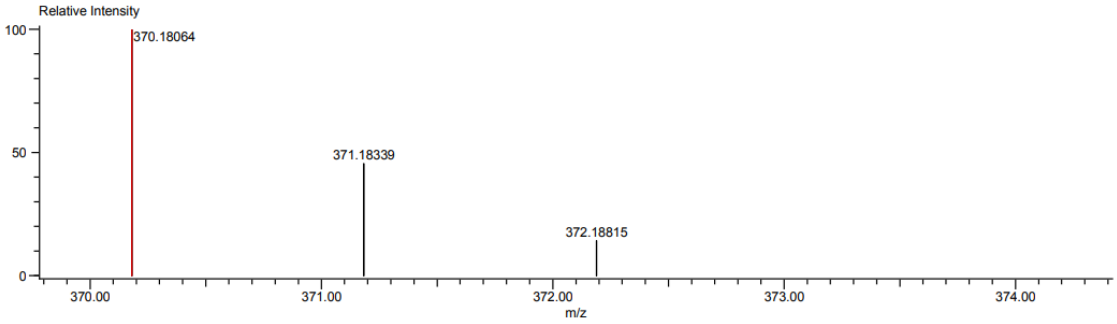

Mass	Intensity	Calc. Mass	Mass Difference (mmu)	Mass Difference (ppm)	Possible Formula	Unsaturation Number
370.18064	35997.67	370.18070	-0.06	-0.16	$^{12}C_{25}{}^{1}H_{24}{}^{14}N_{1}{}^{16}O_{2}$	14.5

Figure S21. High-resolution mass spectrum (DART+) of **AztecNernst-ψ**

4. Absorption and emission fluorescence spectra

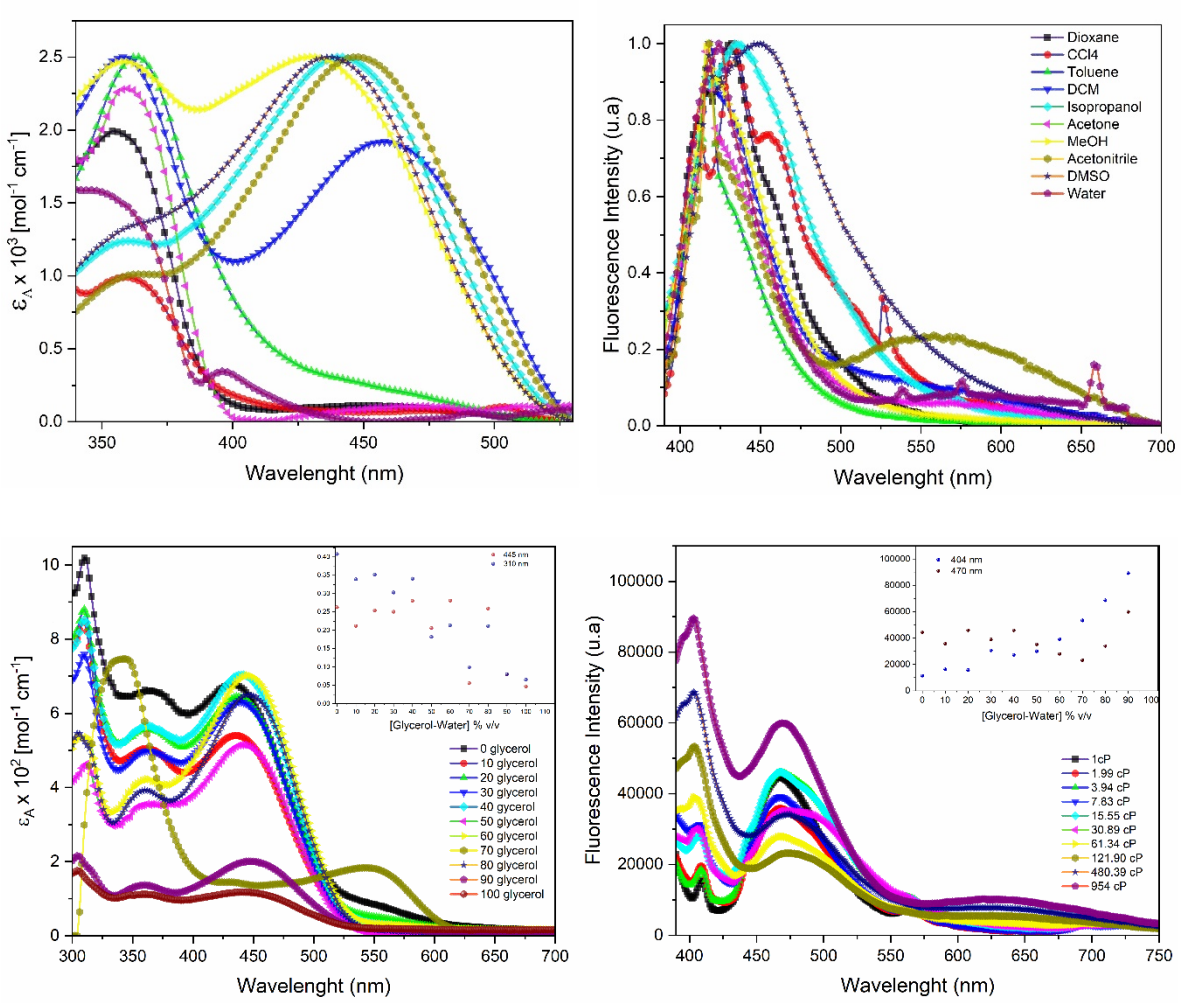

Figure S22. UV-Vis and fluorescence (λ_{exc} = 390 nm) spectra of 40 μM **AN-1** in different solvents. The Panels below show the corresponding UV-Vis and fluorescence spectra of **AN-1** in glycerol/water mixtures varying viscosity from 1 cP to 954 cP.

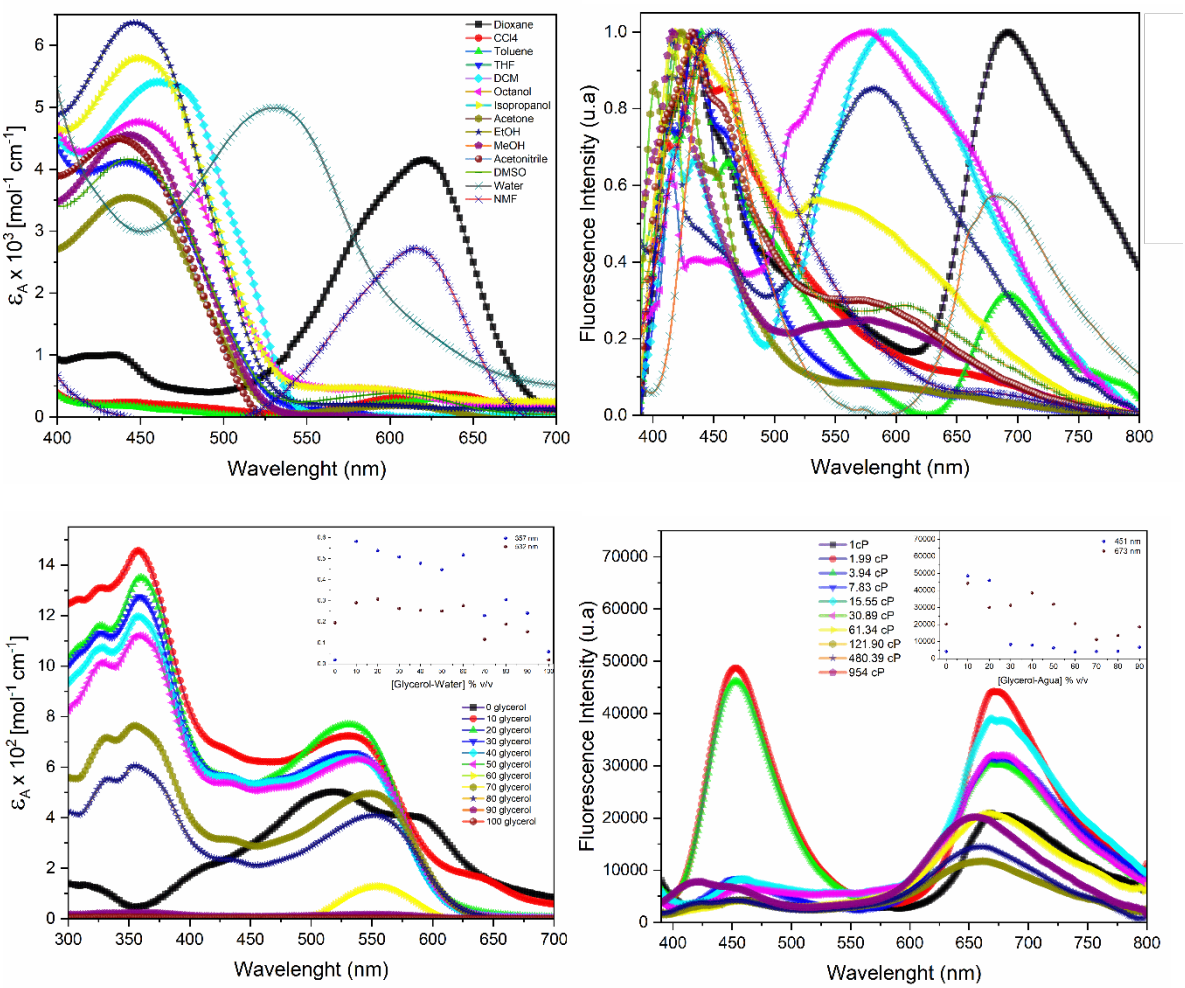

Figure S23. UV-Vis and fluorescence (λ_{exc} = 390 nm) spectra of 40 μM **AN-2** in different solvents. The Panels below show the corresponding spectra in glycerol/water mixtures varying viscosity from 1 cP to 954 cP.

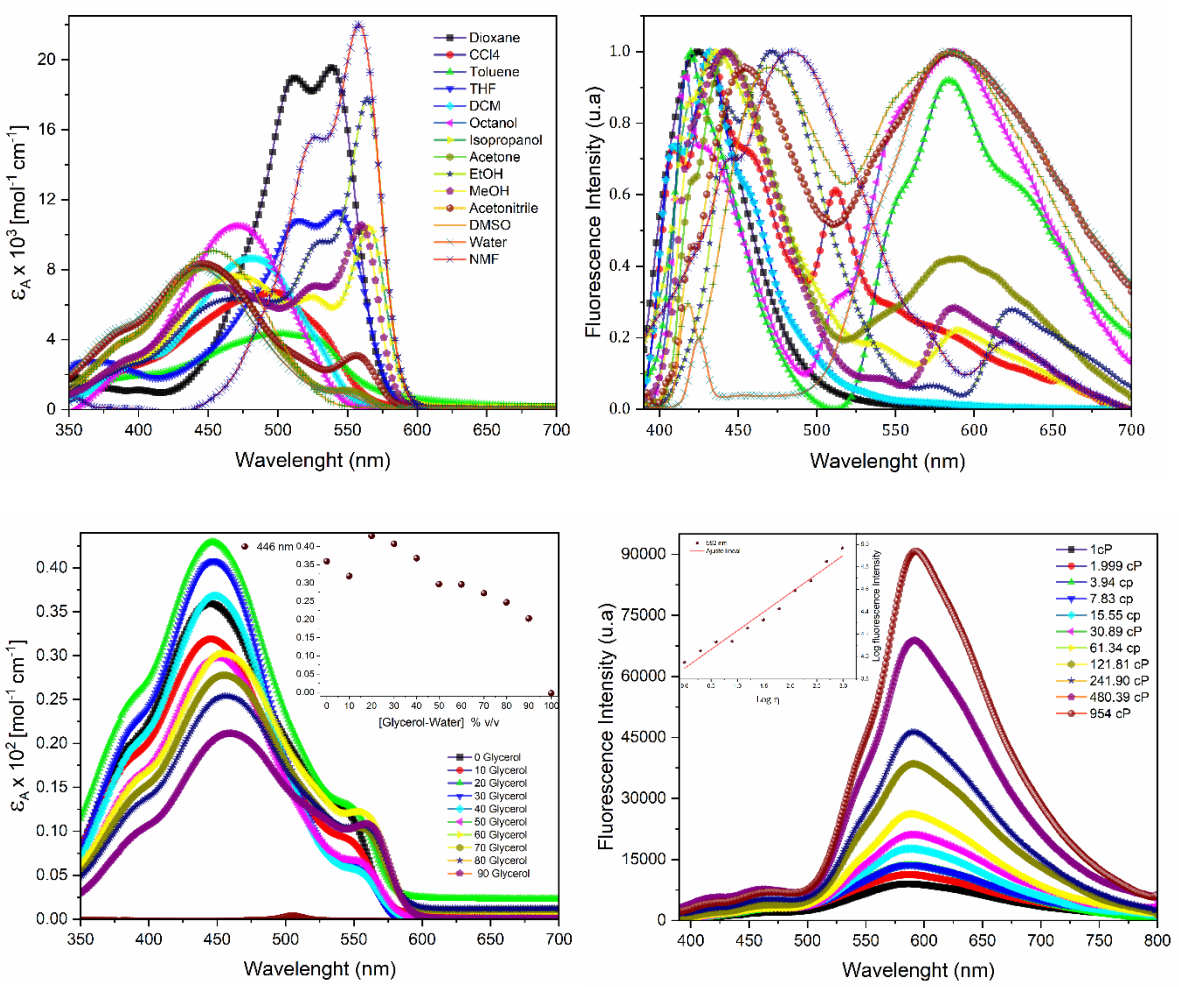

Figure S24. UV-Vis and fluorescence (λ_{exc} = 390 nm) spectra of 40 μM **AN-3** in different solvents. The Panels below show the corresponding UV-Vis and fluorescence spectra of **AN-3** in glycerol/water mixtures varying viscosity from 1 cP to 954 cP.

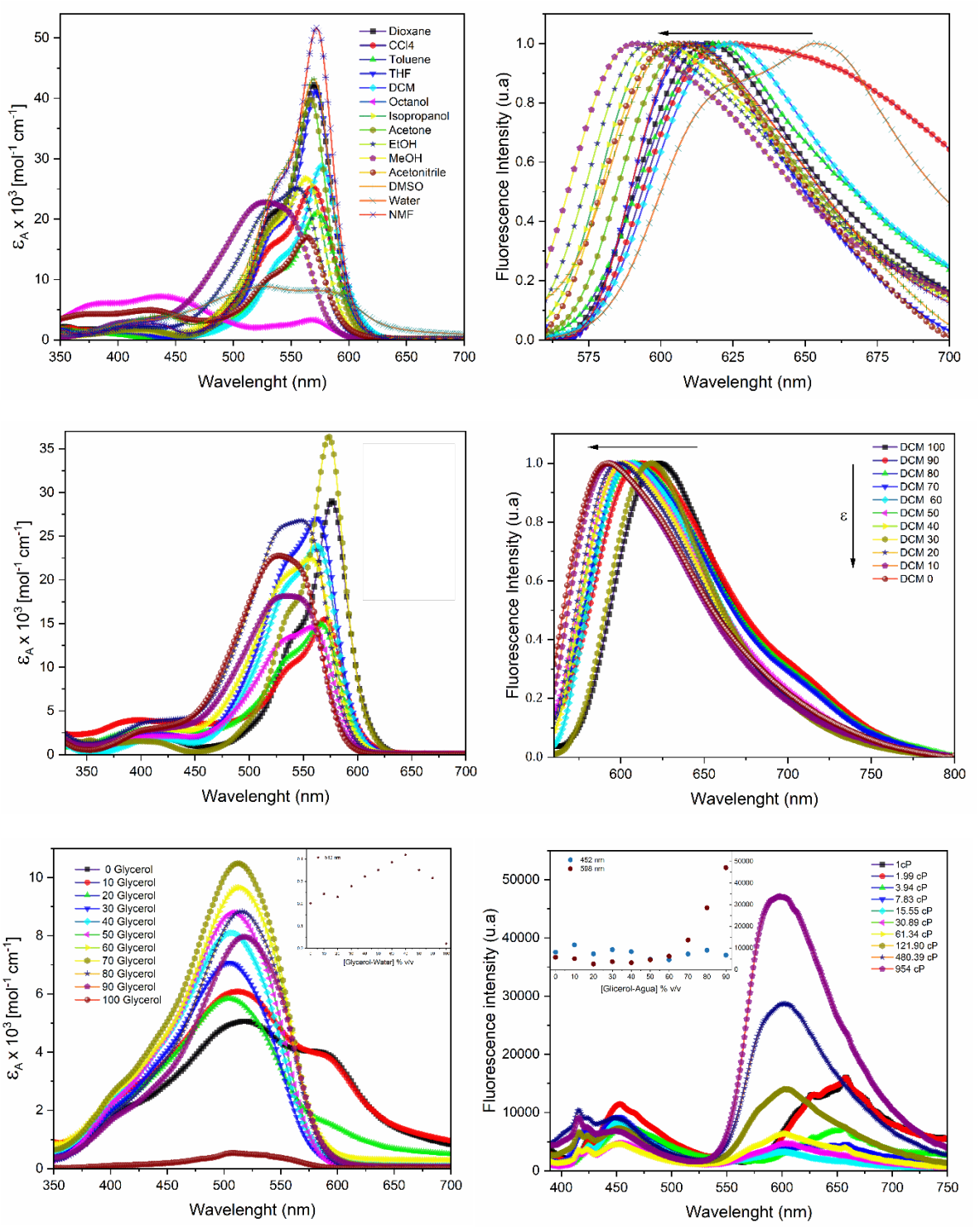

Figure S25. UV-Vis and fluorescence (λ_{exc} = 550 nm) spectra of 40 μM **AN-P** in different solvents and in DCM/methanol mixtures. The Panels below show the corresponding spectra in glycerol/water mixtures varying viscosity from 1 cP to 954 cP.

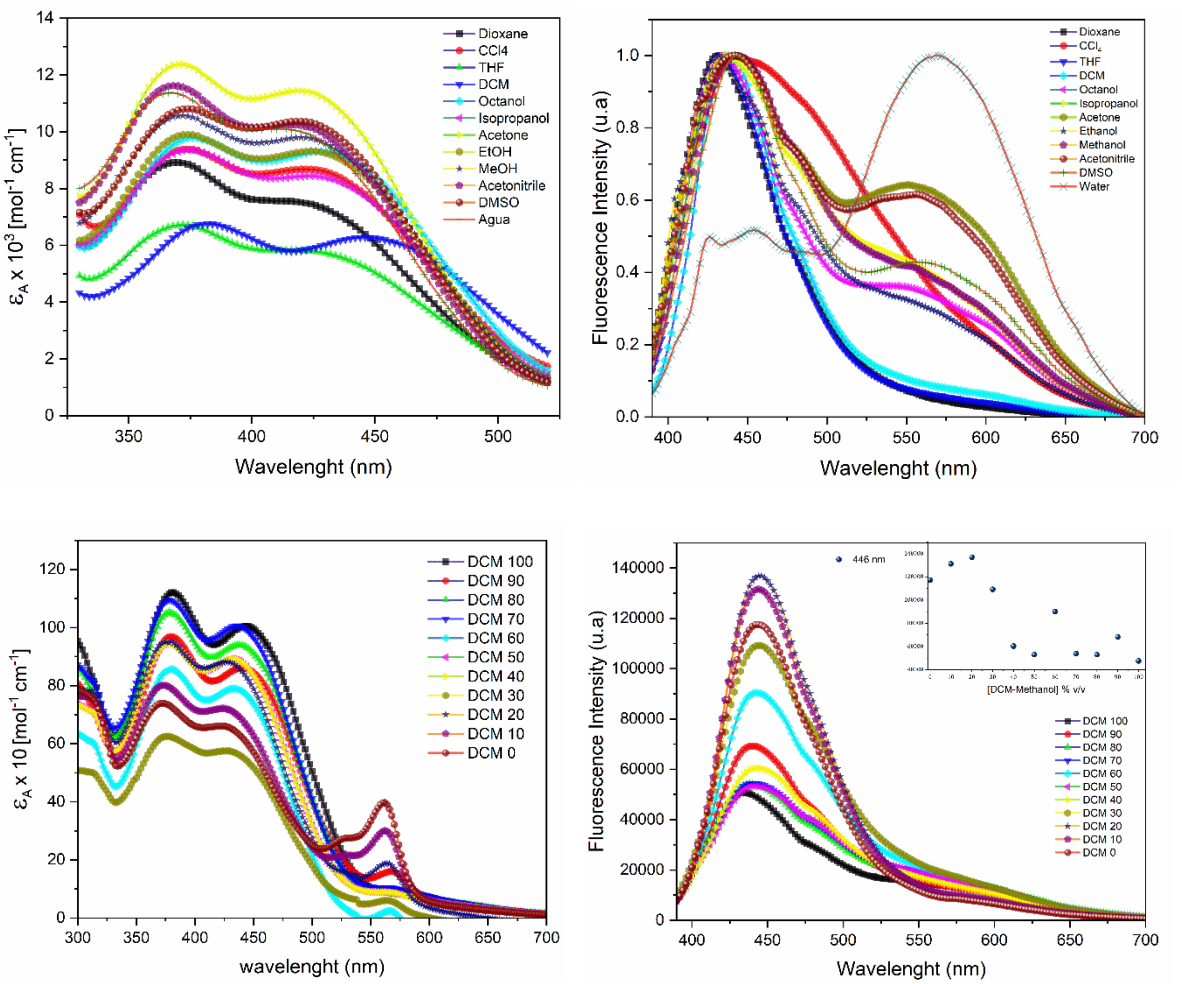

Figure S26. UV-Vis and fluorescence (λ_{exc} = 390 nm) spectra of 40 μM **AztecNernst-ψ** in different solvents and Panels below show the corresponding spectra in DCM-methanol mixtures.

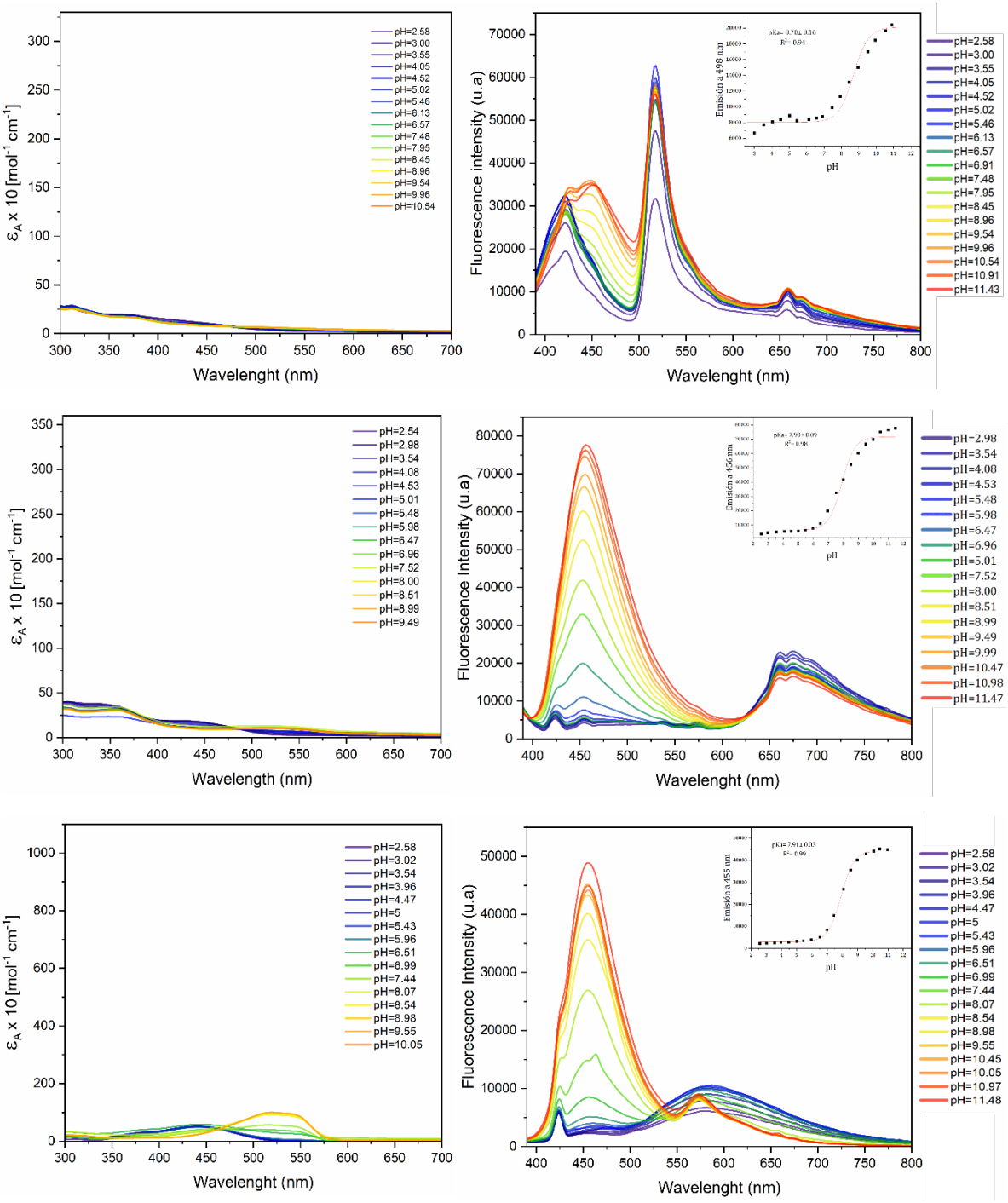

Figure S27. UV-Vis and fluorescence (λ_{exc} = 550 nm) spectra of 40 μM **AN-1**, **AN-2** and **AN-3** at variable pH.

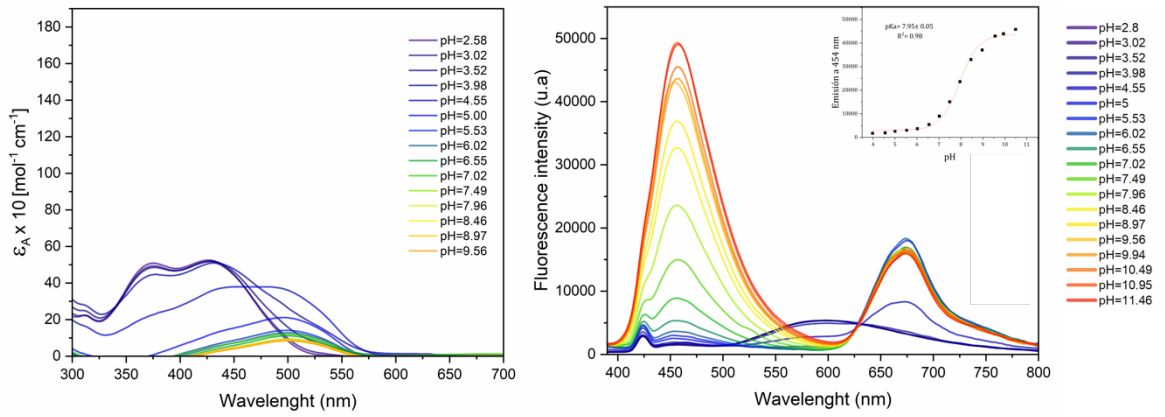

Figure S28. UV-Vis and fluorescence (λ_{exc} = 550 nm) spectra of 40 μM **AN-P**, at variable pH.

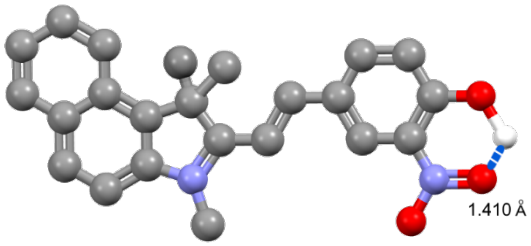

Figure S29. Geometry optimization of **AztecNernst-P** computed at *PBE0/6-31+G(d,p)/IEFPCM-water* level of theory in Gaussian09 program. Hydrogen atoms other than ortho-OH group were removed for clarity. Calculated hydrogen bond [NO-O···H-O] distance is 1.410 Å.

5. Confocal microscopy

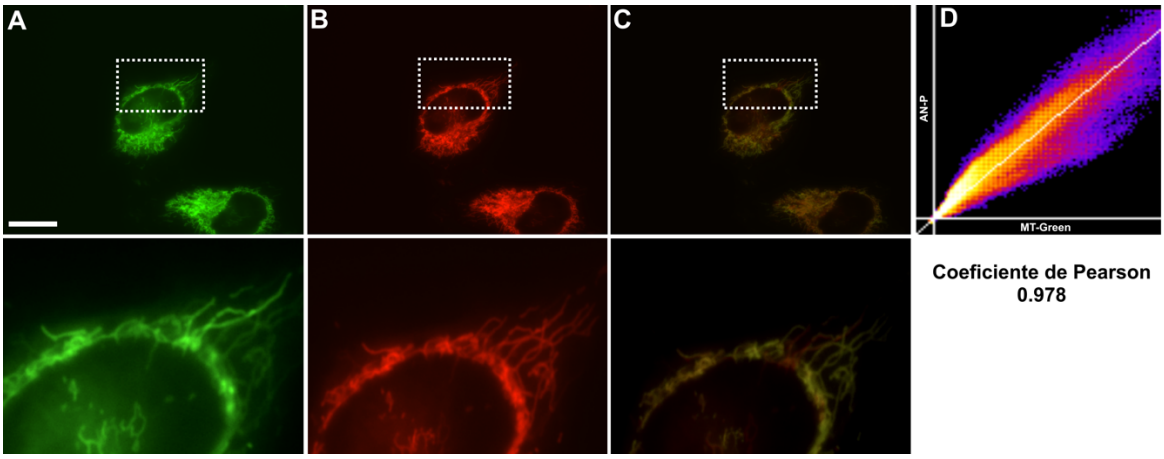

Figure S30. Colocalization imaging of 2 μM **AN-3** using 2 μM MitoLite Blue (λ_{exc} = 410 nm), Pearson's coefficient = 0.978, respectively.

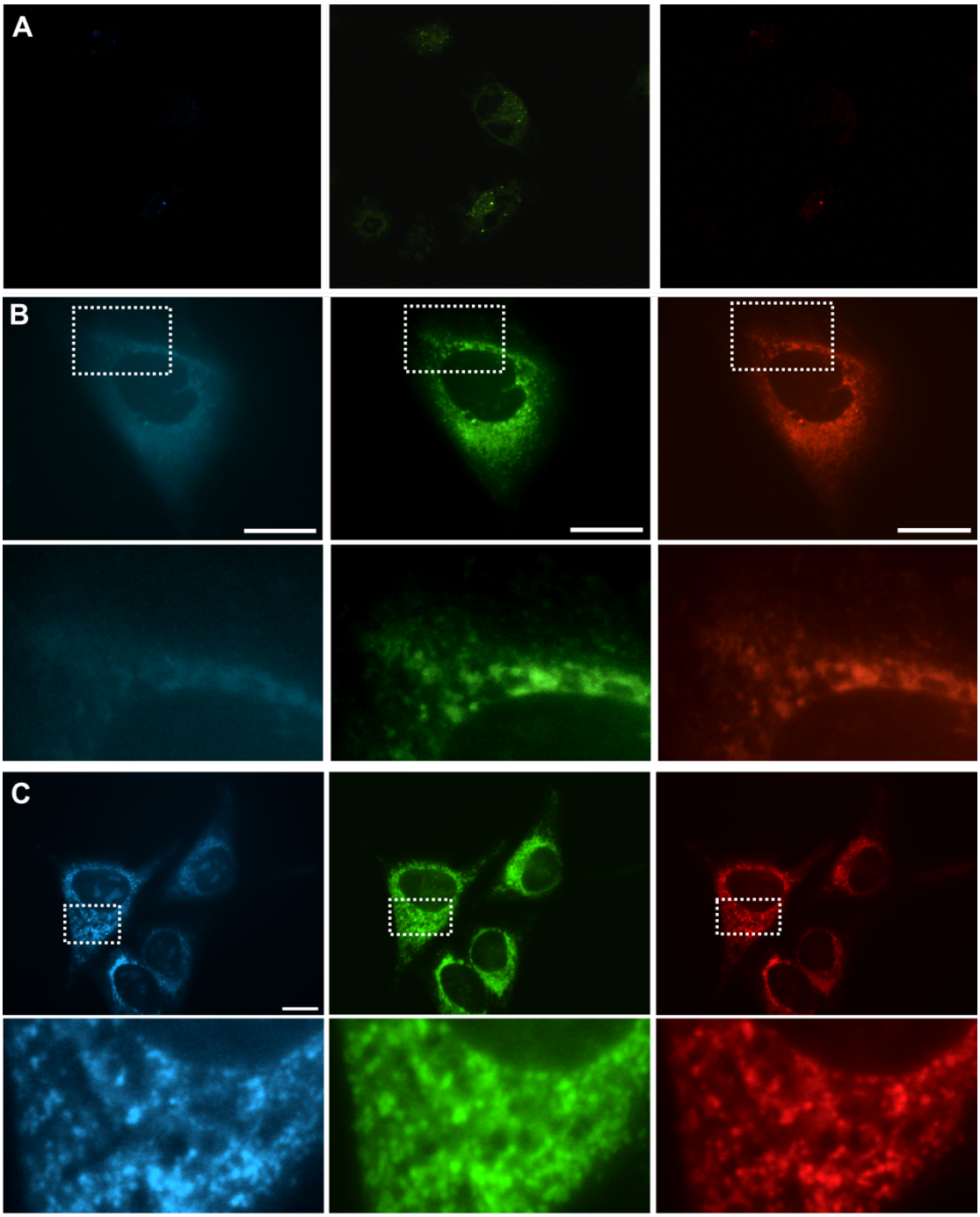

Figure S31. Confocal images of A) **AN-1**, B) **AN-2** and C) **AN-3** fluorescent probes in live U251 cells, stained for 30 min and recorded under the blue (DAPI, λ_{em} = 420–440 nm), green (GFP, λ_{em} = 450–510 nm) and orange-red (TxR, λ_{em} = 620–670 nm) confocal channels. Scale bars represent 20 μm.

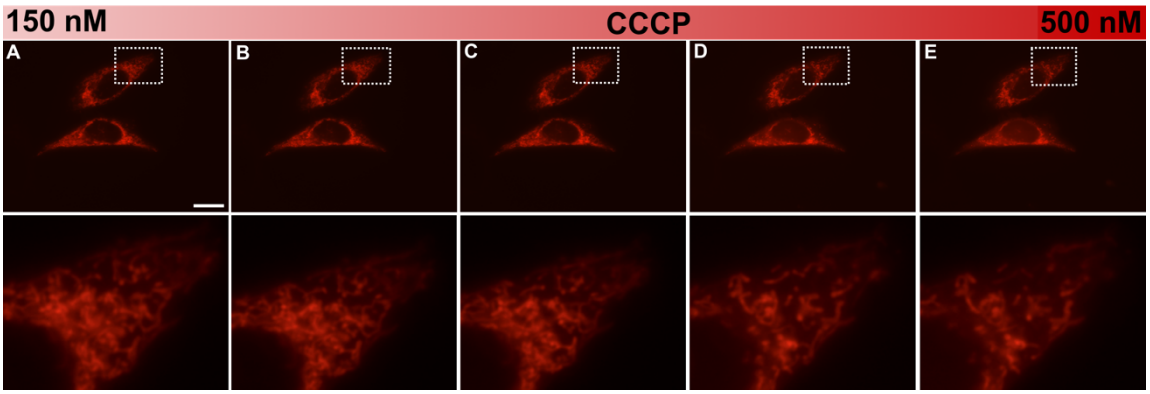

Figure S32. Time course monitoring of CCCP depolarization changes in U251 cells detected in the TxR confocal channel (λ_{exc} = 540 nm) stained with **AN-3** showing a Nernstian behavior or dye release. Then, images were recorded after each 5 min with corresponding CCCP additions from A) 150 nM to E) 500 nM. Scale bar represents 20 μm.

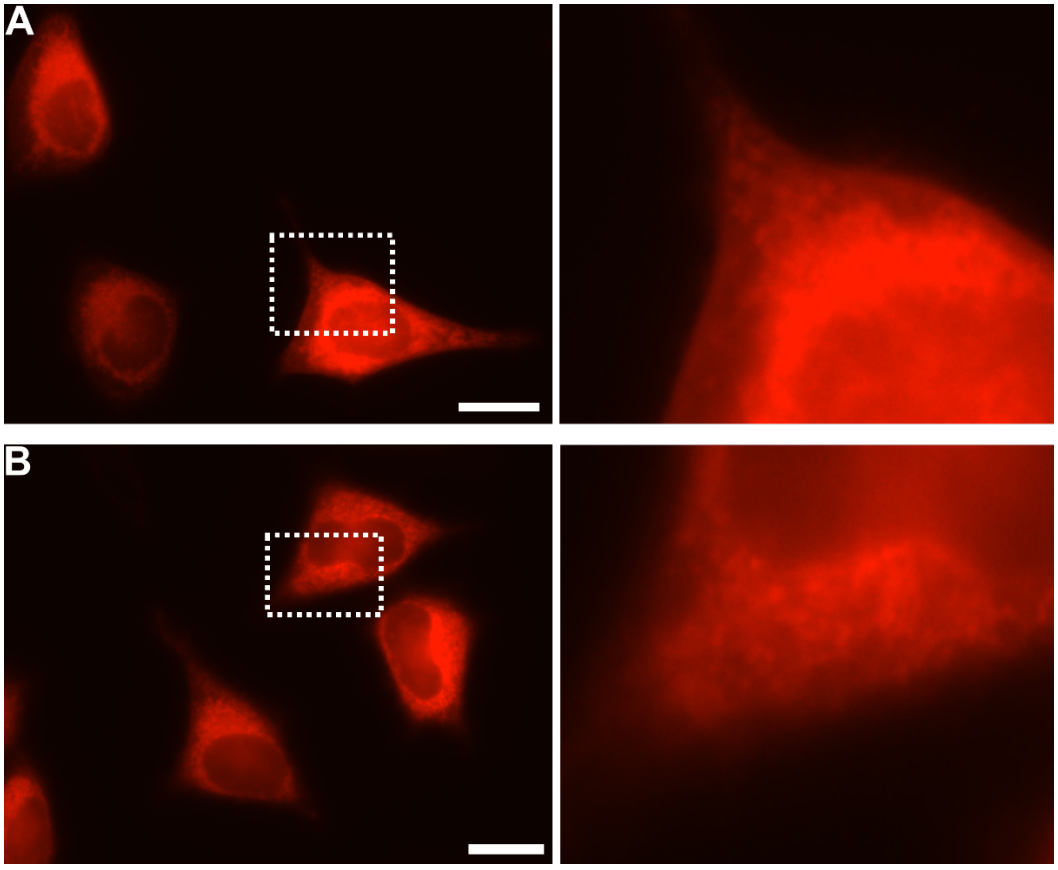

Figure S33. Confocal images of **AztecNernst-ψ** in live U251 cells, (A) stained for 30 min and recorded under the orange-red (TxR, λ_{em} = 620–670 nm) channel and (B) under 10 μg/mL esterases stimuli for 30 min more, where no dye distribution changes are observed. Scale bars represent 20 μm.

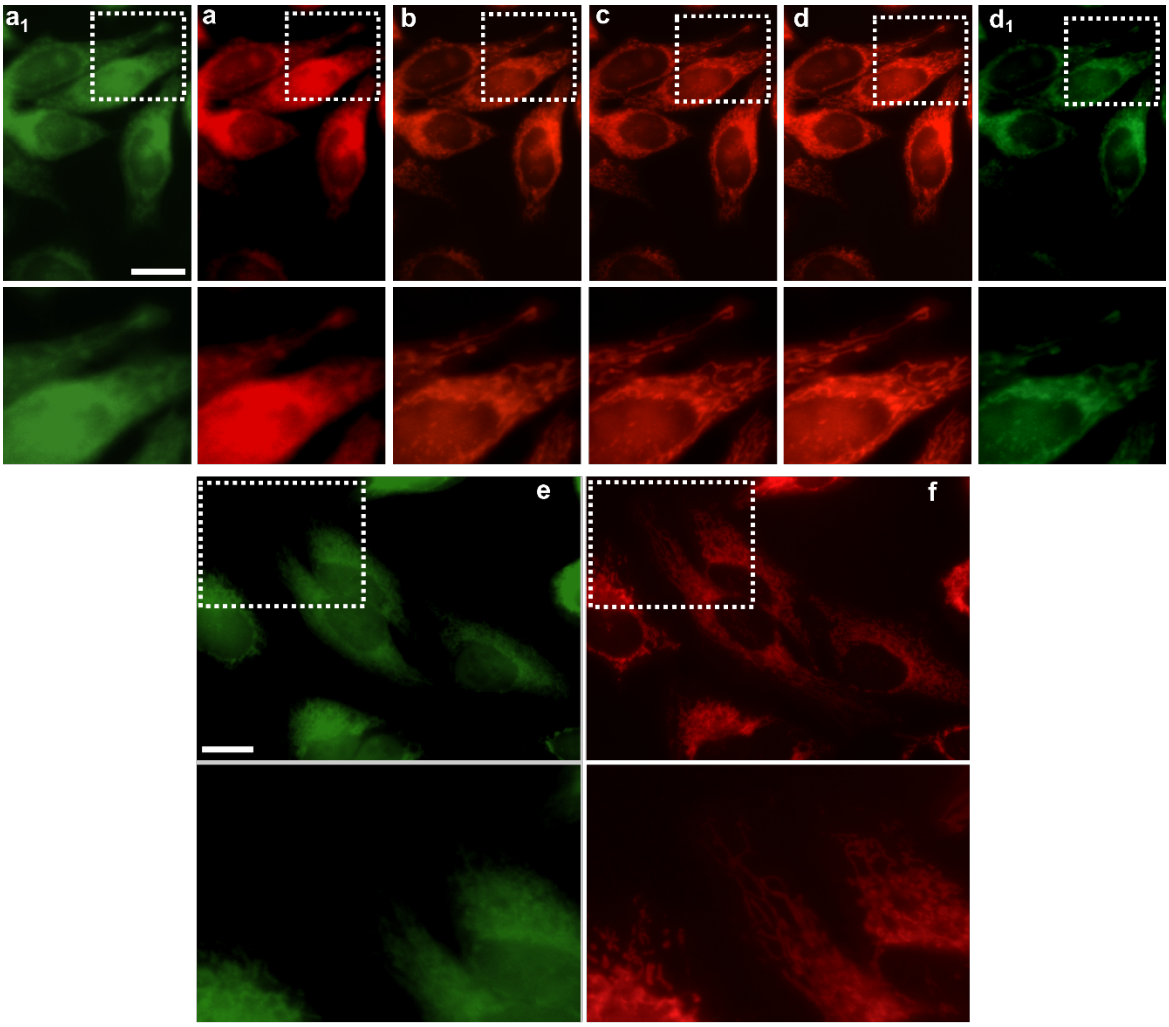

Figure S34. Confocal images of **AztecNernst-P** in U251 cells recorded at the green (λ_{exc} = 480 nm, λ_{em} = 500 nm) and TxR (λ_{exc} = 640 nm, λ_{em} = 680 nm) channels and merged images. Panels **a** to **d** represent the effect of time when the concentration was increased from (a_1 and a) 5 μM; (b) 6 μM; (c) 8 μM and (d and d_1) 10 μM. Panels e and f represent the dual-channel partitioning upon fluorophore concentration increments of 5 to 10 μM. Scale bars represent 20 μm.

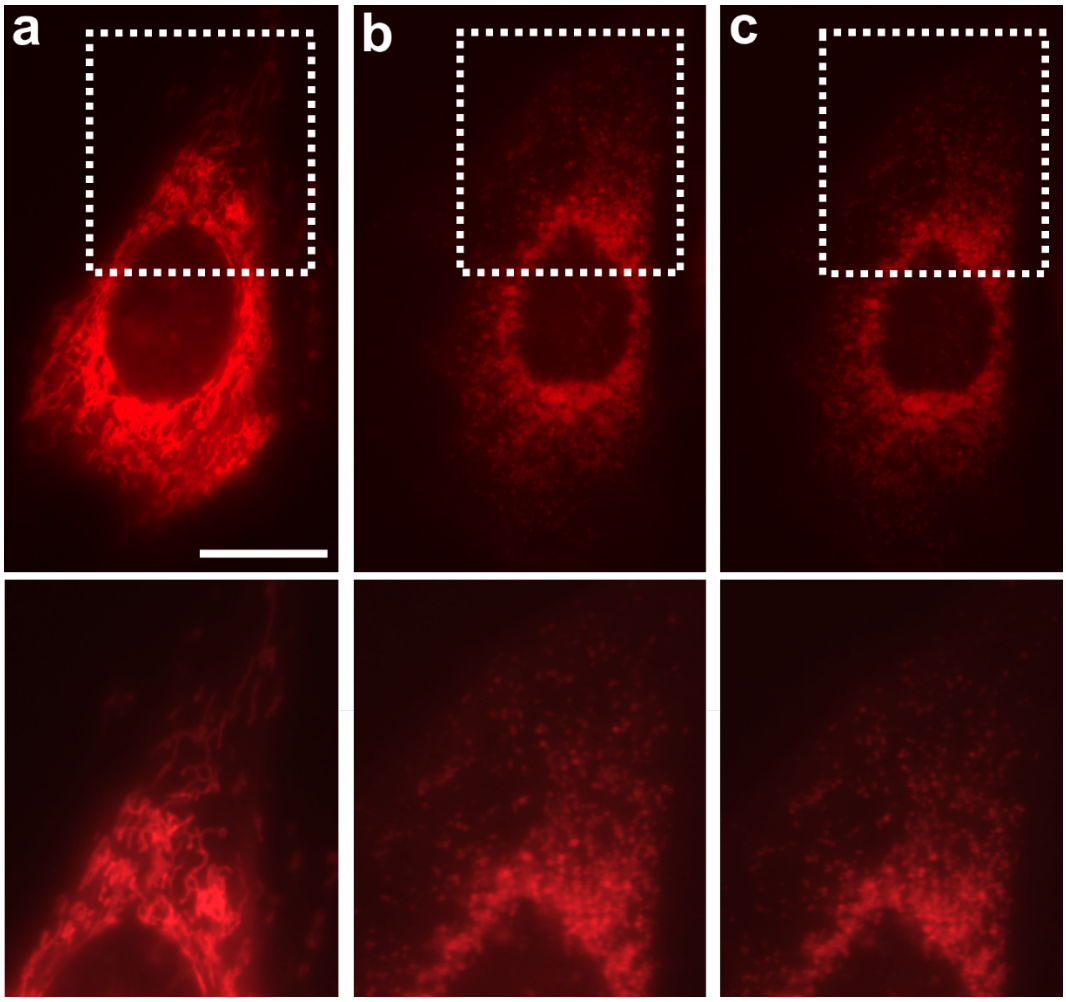

Figure S35. Imaging microscopy of UV-irradiation stimuli impact on mitochondrial dynamics stained with **AztecNernst-P**, initial cell state depicts healthy filamentous-like mitochondrial network (a) and 10 min (b) to 30 min (c) irradiation time leads to sphere morphology, highlighting the stability of **AztecNernst-P** to continuously follow the mitochondrial stress monitoring.

6. Acknowledgements

Financial support by Conacyt Grant No. PCC-319214 is greatly acknowledged. J.O.-H. acknowledges Conahcyt postdoctoral fellowship CVU: 443298, D.C.A acknowledges Conahcyt scholarship to CVU: 1177452. We also acknowledge the assistance of Ruth Rincón Heredia (PhD. Unidad de Imagenología del IFC-UNAM) in imaging microscopy, Adriana Romo Pérez, Ph.D. and Teresa Ramírez Apán, M.Sc. in tissue culture and Everardo Tapia Mendoza (Ph.D., for HRMS studies), Dra. Martha Elena García Aguilera (PhD., for 700 MHz NMR), Elizabeth Huerta Salazar, (M.Sc., for NMR) and Beatriz Quiróz García, (PhD. NMR lab: LURMN at IQ-UNAM) which is funded by CONACYT Mexico (0224747), and UNAM".